J. Mech. Phys. Solids 191 (2024) 105764

Contents lists available at ScienceDirect

Journal of the Mechanics and Physics of Solids

journal homepage: www.elsevier.com/locate/jmps

Stretch-independent magnetization in incompressible isotropic hard magnetorheological elastomers ☆

Kostas Danas [a,b,*], Pedro M. Reis [c,**]

[a] LMS, CNRS, École Polytechnique, Institut Polytechnique de Paris, Palaiseau, 91128, France
[b] ELyTMaX, CNRS, Tohoku University, Sendai, Japan
[c] Flexible Structures Laboratory, Institute of Mechanical Engineering, École Polytechnique Fédérale de Lausanne (EPFL), 1015 Lausanne, Switzerland

ARTICLE INFO

Keywords:
Magnetorheological elastomers
Hard magnetic
Finite-strains
Magnetic dissipation
Elastica
Magnetization

ABSTRACT

Recent studies on magnetically hard, particle-filled magnetorheological elastomers (*h*-MREs) have revealed their stretch-independent magnetization response after full pre-magnetization. We discuss this phenomenon, focusing on incompressible, isotropic, particle-filled *h*-MREs. We demonstrate that the fully dissipative model of Mukherjee et al. (2021) for arbitrary loads can be reduced, under physically consistent assumptions, to the energetic model of Yan et al. (2023), but not that of Zhao et al. (2019). The latter two are valid for small magnetic fields around an already *known* pre-magnetized state. When the pre-magnetized *h*−MRE undergoes non-negligible stretching, the Zhao et al. (2019) model yields predictions that disagree with experiments due to its inherent stretch-dependent magnetization response. In contrast, the Mukherjee et al. (2021) and Yan et al. (2023) models are able to accurately capture this important feature present in pre-stretched *h*-MREs. However, for inextensible slender structures under bending deformation, where stretching is negligible, the Zhao et al. (2019) model provides satisfactory predictions despite its underlying assumptions. Our analysis reveals that, in the fully dissipative model, magnetization can be related to an internal variable but cannot be formally used as one, except for ideal magnets, and is subject to constitutive assumptions. Furthermore, the magnetization vector alone is insufficient to describe the magnetic response of an MRE solid; the introduction of one of the original Maxwell fields is necessary for a complete representation.

1. Introduction and problem definition

In light of the recently burgeoning interest in magneto-mechanical materials, a plethora of theoretical, numerical, and experimental studies have emerged in the literature on magnetically soft (*s*-) and hard (*h*-) magnetorheological elastomers (MREs), also known as magnetoactive elastomers or polymers. In the laboratory, and with some exceptions (Bednarek, 2006; Wang and Gordaninejad, 2009; Gong et al., 2013), three major classes of MREs have been fabricated: *s*-MREs containing carbonyl-iron particles (or other low dissipative ferromagnetic particles), *h*-MREs comprising magnetically dissipative particles (such as NdFeB or similar), and hybrid MREs combining both types of particles. In most cases, the micron-sized particles are in the form of a powder and have fairly

☆ This paper is dedicated to Nicolas Triantafyllidis – who introduced both of us several years ago to the subject of magnetorheological elastomers – on the occasion of his 70th birthday.

* Corresponding author at: LMS, CNRS, École Polytechnique, Institut Polytechnique de Paris, Palaiseau, 91128, France.
** Corresponding author.
E-mail addresses: konstantinos.danas@polytechnique.edu (K. Danas), pedro.reis@epfl.ch (P.M. Reis).

https://doi.org/10.1016/j.jmps.2024.105764
Received 28 February 2024; Received in revised form 3 June 2024; Accepted 30 June 2024
Available online 2 July 2024

spherical or polyhedral shapes (Schümann et al., 2017; Chang et al., 2023). Furthermore, during fabrication, degassing of the mixture is carried out allowing the increase of the total particle volume fraction in the MRE and an overall incompressible response. This study concerns such incompressible MREs, which exhibit enhanced magnetostriction and magnetization response together with sufficiently stiff mechanical response.

The *s*-MREs exhibit high magnetic permeability and magnetization saturation but demagnetize immediately after removal of the magnetic field (Danas et al., 2012). By contrast, *h*-MREs have a significant magnetic coercivity and smaller magnetic saturation but retain their magnetization upon removal of the magnetic field (Stepanov et al., 2017). At this pre-magnetized state, however, *h*-MREs usually exhibit a relatively low magnetic permeability, close to unity. Soft- and hard-magnetic particles can be combined in a matrix, yielding a new class of hybrid MREs (Stepanov et al., 2017; Moreno-Mateos et al., 2022b), that combine, in a non-trivial manner, the individual advantages of *s*-MREs and *h*-MREs and improve the coupled magneto-mechanical response. With the exception of *s*-MREs, which can be cured under a magnetic field to form particle chains and thus exhibit mechanical and magnetic anisotropy (Danas et al., 2012; Danas and Triantafyllidis, 2014), the majority of the magnetoactive material systems fabricated and used to date tend to be mostly isotropic, appearing also nearly homogeneous at the macroscopic scale owing to the micron size of the particles.

Here, we discuss a critical observation relevant to isotropic incompressible *h*-MREs focusing on the *experimentally observed* stretch-independence of the magnetic response of these materials after full pre-magnetization. During the past decade, several studies, theoretical (Mukherjee et al., 2021a) and experimental (Yan et al., 2021, 2023) for isotropic *h*-MREs (see also Danas et al. (2012) for particle-chain *s*-MREs), have demonstrated that the amplitude of the magnetization is independent of the stretching (or stressing) of the material. This finding distinctly opposes the well-known magneto-mechanical Villari effect observed in the context of pure metallic polycrystalline magnets (Kuruzar and Cullity, 1971; Daniel et al., 2014), where the application of stress leads to a change of the magnetization response, both the magnetic permeability and magnetization saturation of the magnet. By contrast, the stretch independence of MREs has important consequences for their response when actuated by external magnetic fields.

In the past few years, numerous studies on *h*-MREs have made extensive usage of the Zhao et al. (2019) model, which has been mainly tested against experimental data on slender structures subjected to *pure* bending and in the absence of any mechanical pre-stresses or pre-stretches (at least of a non-negligible amplitude). In that model and several studies thereafter, the authors make the assumption that the initial pre-magnetization, or, more precisely, remanent magnetic flux, transforms with the deformation gradient. This assumption directly implies that the magnetization of the *h*-MRE will change upon application of tensile or compressive loads, which, as we shall review below, is not supported by recent (Yan et al., 2023) and earlier (Danas et al., 2012) experimental and numerical studies (Mukherjee et al., 2021a). By contrast, the models of Mukherjee et al. (2021a), Mukherjee and Danas (2022) and Yan et al. (2021, 2023) for *h*-MREs and the former models of Danas et al. (2012), Lefèvre et al. (2017) and Mukherjee et al. (2020) for *s*-MREs account for this stretch independence of the magnetization response to a fair extent and, thus, are able to describe cases with non-zero pre-stresses and pre-stretches in a predictive manner.

The main focus of the present study is to closely examine and clarify the similarities and differences between (i) the simpler uncoupled models of Yan et al. (2023) and Zhao et al. (2019) for *h*-MREs and small magnetic loads around the pre-magnetization state and (ii) the fully dissipative coupled model of Mukherjee et al. (2021a). The latter is pertinent for both *s*-and *h*-MREs as well as magneto-mechanical loads of arbitrary amplitude. By coupled and uncoupled magneto-mechanical response, we refer to the ability of the model to predict intrinsic magnetostriction of an MRE under Eulerian applied magnetic fields in the sense described by Danas (2017) and clearly discussed in Section 4. More importantly, we will show that under certain, physically sound assumptions, the Mukherjee et al. (2021a) model may be reduced to the Yan et al. (2023) model but not that of Zhao et al. (2019).

Our manuscript is organized as follows. In Section 2, we introduce the main mechanical and magnetic quantities needed for the analysis of the magneto-mechanical problem. In Section 3, we recall, briefly and concisely, the main ingredients of the fully dissipative model of Mukherjee and Danas (2022) in the **F**-**B** space, which is an exact Legendre dual of the original model of Mukherjee et al. (2021a) that was proposed in the **F**-**H** space. Here, **F** denotes the deformation gradient, while **B** and **H** are the Lagrangian magnetic flux and field strength, respectively. In Section 4, we simplify, under physically sound assumptions, the previous fully dissipative model to two simpler coupled and uncoupled energetic models for *h*-MREs, both of which are valid for small applied magnetic fields around the pre-magnetized state. Then, we summarize the *h*-MRE model of Yan et al. (2023), showing that it turns out to be identical to the uncoupled energetic model of the present study. We proceed by discussing connections and differences between the former two rotation-based models and the Zhao et al. (2019) model. Finally, we close by discussing the limitations of the simpler models as well as the effect that the modeling of the surrounding air has on the response of the MRE.

2. Preliminary definitions

We consider a magneto-mechanical deformable solid that occupies a region $\mathcal{V}_0$ (or $\mathcal{V}$) with boundary $\partial\mathcal{V}_0$ (or $\partial\mathcal{V}$) of outward normal $\mathcal{N}$ (or $\mathbf{n}$) in the undeformed stress-free (or current) configuration. Our analysis is restricted to quasi-static loading conditions and we neglect mechanical body forces and viscoelastic effects. However, many of the points made in this work remain valid in the more general case of viscoelastic materials (see, for example, recent works by Rambausek et al. (2022) and Stewart and Anand (2023)). Material points in the solid are identified by their initial position vector $\mathbf{X}$ in the undeformed configuration $\mathcal{V}_0$, while the current position vector of the same point in the deformed configuration $\mathcal{V}$ is given by $\mathbf{x} = \mathbf{y}(\mathbf{X}) = \mathbf{X} + \mathbf{u}(\mathbf{X})$, with $\mathbf{u}$ denoting the displacement vector. Motivated by the usual physical arguments, the mapping $\mathbf{y}$ is required to be continuous and one-to-one on $\mathcal{V}_0$. In addition, we assume that $\mathbf{y}$ is twice continuously differentiable, except, possibly, on existing interfaces (*e.g.*, due to the presence of different phases) inside the material. The deformation gradient and its polar decomposition is then denoted by

$$\mathbf{F} = \mathrm{Grad}\mathbf{y} = \mathbf{I} + \mathrm{Grad}\mathbf{u}, \qquad \mathbf{F} = \mathbf{R}\mathbf{U}, \quad \mathbf{R}^T\mathbf{R} = \mathbf{R}\mathbf{R}^T = \mathbf{I}, \quad \mathbf{U}^T = \mathbf{U}. \tag{1}$$

In this expression, $\mathbf{R}$ is an orthogonal tensor, $\mathbf{U}$ is the right stretch (symmetric) tensor and $\mathbf{I}$ the second-order identity tensor. Its determinant is positive, i.e., $J = \det \mathbf{F} > 0$ to impose the impenetrability condition. Moreover, "Grad" denotes the gradient operator with respect to $\mathbf{X}$ in the reference configuration. In addition, the reference density of the solid ρ_0 is related to the current density ρ by $\rho_0 = \rho J$.

Traditionally, in the absence of electric currents and charges, the following three quantities are used to describe the magnetic state of a solid in the *current* configuration:

- the current magnetic flux $\mathbf{b}$;
- the current magnetic field strength $\mathbf{h}$; and
- the current magnetization $\mathbf{m}$, which, by construction, is zero in non-magnetic domains.

It is important to note, however, that these three quantities are not independent of one another; they are related by the *constitutive* relation $\mathbf{b} = \mu_0(\mathbf{h} + \mathbf{m})$, which may be recast as

$$\mathbf{m} = \frac{1}{\mu_0}\mathbf{b} - \mathbf{h} \qquad \text{in} \quad \mathcal{V}, \tag{2}$$

with μ_0 denoting the magnetic permeability of vacuum, air, or non-magnetic solids.

Remark 1. In fact, the expression in Eq. (2) is a *definition* of the magnetization vector in the *current* volume $\mathcal{V}$, which, however, is not defined on its boundary $\partial\mathcal{V}$, and does not have a unique Lagrangian definition (Dorfmann and Ogden, 2004). Moreover, by definition, $\mathbf{m} = \mathbf{0}$ in a non-magnetic body. This statement implies that $\mathbf{m}$ is insufficient as a variable to describe the presence of magnetic lines (in the sense of Maxwell) in the surrounding air or in the non-magnetic medium more generally (*e.g.,* a polymer), two settings that are commonly of interest in most problems involving magnetic materials. In these two cases, one is left with the relation $\mathbf{b} = \mu_0\mathbf{h}$, which implies (in the sense of a continuum medium) that $\mathbf{b}$ is linearly dependent on $\mathbf{h}$, and *vice versa*, via the magnetic constitutive parameter μ_0. Henceforth, we seek to reconcile, in certain special cases, the approaches using the original Maxwell fields $\mathbf{b}$ and $\mathbf{h}$ (or their Lagrangian counterparts discussed below) as working variables (Dorfmann and Ogden, 2003) and those using all three, $\mathbf{b}$, $\mathbf{h}$, and $\mathbf{m}$ (Brown, 1963; James and Kinderlehrer, 1993; Kankanala and Triantafyllidis, 2004). Moreover, in Section 4, we will show that $\mathbf{m}$, unlike the original Maxwell fields $\mathbf{b}$ and $\mathbf{h}$, can be related to an internal–and not an independent–variable that describes permanent magnetization states in the MRE solid.

At large strains, the fields $\mathbf{b}$ and $\mathbf{h}$ can be pulled back from $\mathcal{V}$ to $\mathcal{V}_0$ to their Lagrangian forms, denoted by $\mathbf{B}$ and $\mathbf{H}$, respectively, such that (Dorfmann and Ogden, 2003; Kankanala and Triantafyllidis, 2004; Bustamante et al., 2008)

$$\mathbf{B} = J\mathbf{F}^{-1}\mathbf{b}, \qquad \text{and} \qquad \mathbf{H} = \mathbf{F}^T\mathbf{h}. \tag{3}$$

Moreover, as has been extensively discussed in the literature (see, for instance, Dorfmann and Ogden (2005)), Eq. (2) is not form invariant under transformations, which is a manifestation of the non-unique definition of $\mathbf{m}$. The Lagrangian $\mathbf{B}$ is also divergence-free and $\mathbf{H}$ is curl-free, such that

$$\mathrm{Div}\mathbf{B} = 0 \quad \text{in } \mathcal{V}_0, \qquad [\![\mathbf{B}]\!] \cdot \boldsymbol{\mathcal{N}} = 0 \quad \text{in } \partial\mathcal{V}_0^{\mathrm{B}}, \tag{4}$$

and

$$\mathrm{Curl}\,\mathbf{H} = \mathbf{0} \quad \text{in } \mathcal{V}_0, \qquad [\![\mathbf{H}]\!] \times \boldsymbol{\mathcal{N}} = \mathbf{0} \quad \text{on } \partial\mathcal{V}_0^{\mathrm{H}}. \tag{5}$$

The explicit notation $\partial\mathcal{V}_0^{\mathrm{B}}$ and $\partial\mathcal{V}_0^{\mathrm{H}}$ serve to denote the corresponding parts of the boundary where jumps in $\mathbf{B}$ and $\mathbf{H}$ are applied.

The total Cauchy stress tensor $\boldsymbol{\sigma}$ and the total (first) Piola–Kirchhoff $\mathbf{S}$ read, respectively,

$$\boldsymbol{\sigma} = \frac{1}{J}\mathbf{S}\mathbf{F}^T, \quad \text{and} \quad \mathbf{S} = J\mathbf{F}^{-1}\boldsymbol{\sigma}. \tag{6}$$

In the absence of mechanical body forces and dynamic loads, both of these stress measures are divergence-free, for instance,

$$\mathrm{Div}\,\mathbf{S} = \mathbf{0} \quad \text{in } \mathcal{V}_0, \quad \mathbf{S}\mathbf{F}^T = \mathbf{F}\mathbf{S}^T, \quad \text{and} \quad [\![\mathbf{S}]\!] \cdot \boldsymbol{\mathcal{N}} - \mathbf{T} = \mathbf{0} \quad \text{on } \partial\mathcal{V}_0^{\mathrm{T}}, \tag{7}$$

where $\mathbf{T}$ denotes the mechanical traction in the reference configuration applied on the corresponding part of the boundary $\partial\mathcal{V}_0^{\mathrm{T}}$.

3. The magnetic dissipation model of Mukherjee et al. (2021a)

3.1. Internal variable for magnetic dissipation

A thermodynamically consistent model for any dissipative material may be constructed through the definition of a finite number of internal variables, which reflect the irreversible processes the material undergoes under external loads. Those internal variables are, in general, difficult to measure directly in an experiment (*e.g.*, plastic strain, or magnetization), and moreover, they cannot be controlled with direct manipulations (Bassiouny et al., 1988; Eringen and Maugin, 1990). Nevertheless, they are necessary to describe the time evolution of the internal state of the material since they carry information on the history of the processes (*e.g.*, motion of dislocations and domain walls, bypassing or pinning at obstacles). In this regard, one of the main differences between *h*-MREs and *s*-MREs is the underlying magnetic dissipation of the filler particles (*e.g.*, NdFeB) in the former. Upon cyclic magnetic

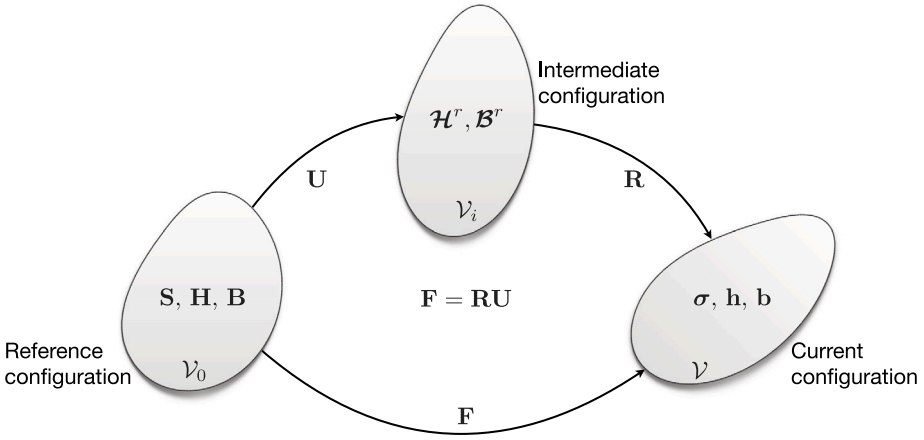

Fig. 1. Definition of the reference, intermediate and current configurations of volume $\mathcal{V}_0$, $\mathcal{V}_i$ and $\mathcal{V}$, respectively, along with the different field variables defined therein.

loading, as a consequence of the finite strains and the magneto-mechanical coupling, the response of the *h*-MRE composite exhibits both magnetic and mechanical hysteresis.

Through the extensive analysis of data from numerical RVE simulations, Mukherjee et al. (2021a) have shown that only one internal remanent H-like[1] vector variable,

$$\boldsymbol{\mathcal{H}}^r \in \mathbb{R}^3, \tag{8}$$

which lies in the *stretch-free*, *intermediate* configuration $\mathcal{V}_i$ (see Fig. 1) suffices to describe the magneto-mechanical behavior of an *incompressible* *h*-MRE. This assumption is not unusual. For example, the analogous classical J_2 flow theory of elasto-plasticity makes a similar assumption for the plastic deformation gradient $\mathbf{F}^p$ (Lee, 1969) or plastic strain $\boldsymbol{\epsilon}^p$ (Hill, 1950).

Remark 2. We note at this point that $\boldsymbol{\mathcal{H}}^r$ is a magnetic variable, independent of the deformation gradient $\mathbf{F}$, and as such implies (see Fig. 1) that one may define a Eulerian remanent field, $\mathbf{h}^r$, that is stretch independent and is given by a push-forward operation, i.e., $\mathbf{h}^r = \mathbf{R}\boldsymbol{\mathcal{H}}^r$, with $\mathbf{R}$ defined in $(1)_2$. Similarly a pull-backward operation may be carried out leading to a Lagrangian remanent field, $\mathbf{H}^r = \mathbf{U}\boldsymbol{\mathcal{H}}^r$, with $\mathbf{U}$ defined again in $(1)_2$. Nevertheless, those measures are non-essential since they cannot be given any particular physical interpretation, and more importantly, given that they are not independent variables, they cannot be measured or directly controlled (Eringen and Maugin, 1990).

A direct consequence of the above unambiguous numerical and theoretical results is that the current magnetization vector, $\mathbf{m}$ (indirectly related to $\boldsymbol{\mathcal{H}}^r$) is affected by macroscopic rotations but not stretches, as we will show in the following sections. These observations are also confirmed experimentally and independently in the works of Yan et al. (2021, 2023) for *h*-MREs and the earlier study of Danas et al. (2012) for *s*-MREs.[2] In particular, Yan et al. (2023) have first employed a three-dimensional (3D) model, based on that of Zhao et al. (2019) (hereon denoted as the **FM**-model with **M** being the pre-magnetization vector), which leads to changes of the magnetization amplitude (and direction) upon application of a deformation gradient. The authors showed that, in some cases where stretching is not negligible, this **FM** model yields unphysical predictions (*i.e.*, in disagreement with experimental data), as they demonstrated for the specific configuration of a thin plate made of an *h*-MRE, actuated under combined mechanical (pressure) and magnetic loading. Following an alternative point of departure, these authors then developed a model (hereon denoted as the **RM**-model), which, upon application of a deformation gradient, $\mathbf{F} = \mathbf{RU}$, imposes changes *solely* in the orientation of the magnetization vector due to the presence of only the rotation part, $\mathbf{R}$, and *not* the stretch part, $\mathbf{U}$. This **RM**-model was found to yield predictions in excellent agreement with experimental data, as we will discuss in more detail in Section 6. Yan et al. (2023) also demonstrated that classical dimensional-reduction techniques to derive equilibrium equations for *inextensible* slender structures (beams, elastica, plates, and shells) that invoke Euler–Bernoulli or Kirchhoff–Love hypotheses for the kinematics (*i.e.*, normals stay normal to the center-line/mid-surface and do not stretch) naturally *block* the stretching and give the erroneous impression that **FM** models are appropriate for such structures made of *h*-MREs. Similarly, but for incompressible, particle-chain *s*-MREs, earlier experimental work by Danas et al. (2012) showed that pre-stressing of the material (even when anisotropic) and upon the application of an external magnetic field, leads to an effectively unchanged amplitude of the magnetization response, albeit strongly affecting its magnetostriction.

[1] Given the arbitrary nature of choosing internal variables, it is evident that one could also have reasonably chosen a B-like variable. Mukherjee and Danas (2022) subsequently showed that such a choice is inconsequential for the analysis and is a mere matter of *taste*.

[2] We recall that the case of *s*-MREs may be recovered in the limit of vanishing dissipation of the *h*-MRE model (Mukherjee and Danas, 2022; Danas, 2024).

The two independent experiments discussed above and reported in Yan et al. (2023) and Danas et al. (2012), together with their respective numerical and theoretical analyses therein, provide unambiguous and convincing evidence that the *amplitude of the magnetization* response of isotropic or particle-chain, *incompressible* particle-filled MREs more generally is insensitive to mechanical stretches. Certainly, considering large shear loads may alter the direction of magnetization, consequently rendering the analysis highly nuanced and intricate. In this context, it is noteworthy that incompressible MREs do not exhibit the inverse magnetoelastic Villari effect of metallic magnets, which do so but are compressible and the applied stresses are of a much higher amplitude (Kuruzar and Cullity, 1971).

In Section 4, we will demonstrate that the current magnetization $\mathbf{m}$ is a function of $\boldsymbol{\mathcal{H}}^r$, implying that $\mathbf{m}$ (or its representation in a different configuration) can be linked directly to an internal variable; cf. the relevant work of Klinkel (2006), Linnemann et al. (2009) and Kalina et al. (2017). However, we will see that failing to use an appropriate transformation of $\mathbf{m}$ can lead to important errors. We will then establish a direct connection between the full dissipative theory of Mukherjee et al. (2021a) and Mukherjee and Danas (2022), as well as the simplified energetic models of Yan et al. (2021, 2023). We emphasize that the latter two studies provided strong experimental evidence for the fact that the current magnetization is stretch-independent and affected only by rotations.

In the remaining of the work, we focus on isotropic, incompressible, particle-filled *h*-MREs.

3.2. The isotropic magneto-mechanical invariants for h-MREs

A natural way to satisfy the conditions of even magneto-mechanical coupling, isotropic material symmetry, and frame indifference is to express the energy density and dissipation in terms of appropriately chosen *isotropic* invariants. In Mukherjee and Danas (2022), a dual formulation in the sense of Legendre–Fenchel was proposed for *h*-MREs, yielding exactly equivalent constitutive laws in both the **F**-**H** and **F**-**B** space. In the present study, we focus on the **F**-**B** formulation, which allows us to make direct contact with Yan et al. (2023), as well as assess the limitations of the earlier model of Zhao et al. (2019). Moreover, for consistency with earlier works by a subset of the authors of these two studies, we will also present a quasi-incompressible version of the models. Note, however, that the formalism we will propose is only valid for minor volume changes and not for general compressible MREs; for the latter, we refer to the recent work of Gebhart and Wallmersperger (2022a,b) on this topic.

First, we will define the general set of available invariants, $\mathbb{C} = \mathbf{F}^T\mathbf{F}$, $\mathbf{B}$, and $\boldsymbol{\mathcal{H}}^r$, given the corresponding arguments. Subsequently, we will select a subset of them to model the *h*-MREs; a choice that is primarily motivated by corresponding numerical RVE simulations of two-phase *h*-MRE composites (Mukherjee et al., 2021a). While this choice does not represent a rigorous result, it serves as an effective homogenization-guided approach. This strategy ensures that the number of invariants remains minimum and keeps the model entirely explicit.

Mechanical invariants.

$$I_1 = \mathrm{tr}(\mathbb{C}), \qquad I_3 = J^2 = \det \mathbb{C} = 1, \tag{9}$$

Magneto-mechanical invariants in **F**-**B** *formulation.*

$$\begin{aligned}
&I_4^{\mathrm{B}} = \mathbf{B}\cdot\mathbf{B}, && I_4^{\mathrm{BHr}} = \mathbf{B}\cdot\mathbb{C}^{-1/2}\boldsymbol{\mathcal{H}}^r, && I_4^{\mathrm{Hr}} = \boldsymbol{\mathcal{H}}^r\cdot\mathbb{C}\boldsymbol{\mathcal{H}}^r\\
&I_5^{\mathrm{B}} = \mathbf{B}\cdot\mathbb{C}\mathbf{B}, && I_5^{\mathrm{BHr}} = \mathbf{B}\cdot\mathbb{C}^{1/2}\boldsymbol{\mathcal{H}}^r, && I_5^{\mathrm{Hr}} = \boldsymbol{\mathcal{H}}^r\cdot\boldsymbol{\mathcal{H}}^r.\\
&I_6^{\mathrm{B}} = \mathbf{B}\cdot\mathbb{C}^2\mathbf{B}, && I_6^{\mathrm{BHr}} = \mathbf{B}\cdot\mathbb{C}^{3/2}\boldsymbol{\mathcal{H}}^r && I_6^{\mathrm{Hr}} = \boldsymbol{\mathcal{H}}^r\cdot\mathbb{C}^2\boldsymbol{\mathcal{H}}^r.
\end{aligned} \tag{10}$$

3.3. Energy densities and dissipation potential

We express the energy density, $W(\mathbf{F},\mathbf{B})$, as the sum of three distinct energy densities, namely, the purely mechanical ($\rho_0\Psi_{\mathtt{mech}}$), purely magnetic ($\rho_0\Psi_{\mathtt{mag}}$) and coupling ($\rho_0\Psi_{\mathtt{couple}}$), such that[3]

$$W(\mathbf{F},\mathbf{B},\boldsymbol{\mathcal{H}}^r) = \rho_0\Psi_{\mathtt{mech}}(I_1,J) + \rho_0\Psi_{\mathtt{mag}}(I_5^{\mathrm{B}}, I_5^{\mathrm{BHr}}, I_5^{\mathrm{Hr}}) + \rho_0\Psi_{\mathtt{couple}}(I_4^{\mathrm{Hr}}, I_5^{\mathrm{BHr}}, I_5^{\mathrm{Hr}}, I_6^{\mathrm{BHr}}) + \frac{1}{2\mu_0 J} I_5^{\mathrm{B}}, \tag{11}$$

where ρ_0 is the reference density of the solid, and the last term ($I_5^{\mathrm{B}}/2\mu_0$) in Eq. (11) represents the energy associated with free space with μ_0 being the magnetic permeability in vacuum or in non-magnetic solids such as the polymer matrix phase. This last term is necessary for mathematical consistency (Dorfmann and Ogden, 2003, 2024) as well as for modeling the effect of the surrounding air upon the MRE body. We also note that in the proposed model in Eq. (11), a subset of the invariants defined in Eq. (10) was found to be sufficient for the problem at hand.

The mechanical energy density. The purely mechanical free energy density $\rho_0\Psi_{\mathtt{mech}}$ in Eq. (11) may be chosen to correspond to the analytical homogenization estimate of Lopez-Pamies et al. (2013) for a two-phase composite made of an incompressible nonlinear

[3] In the original work of Mukherjee and Danas (2022) the notation W^{B} was used to distinguish between the **F**-**B** model and the equivalent dual in the **F**-**H** space denoted with W^{H}. In the present work, we only use the **F**-**B** version, and thus, the relevant superscripts will be dropped for simplicity of the notation. In turn, for clarify, the superscripts will be maintained when writing the invariants.

Table 1
Magnetic properties of the particles.

Volume fraction	Energetic susceptibility	Remanent susceptibility	Magnetization saturation	Coercivity
c [–]	χ_{p}^{e} [–]	χ_{p}^{r} [–]	m_{p}^{s} [MA/m]	b_{p}^{c} [T]

elastic matrix comprising isotropic distributions of rigid-particles, such that

$$\rho_0\Psi_{\mathtt{mech}}(I_1,J)=(1-c)\rho_0\Psi_{\mathtt{m,mech}}(\mathcal{I}_1)+\frac{K_{\mathtt{m}}}{2(1-c)^6}(J-1)^2,\qquad \mathcal{I}_1=\frac{J^{-2/3}I_1-3}{(1-c)^{7/2}}+3, \tag{12}$$

where c is the particle volume fraction, $K_{\mathtt{m}}$ (much larger than the shear modulus) is the compressibility modulus and $\Psi_{\mathtt{m,mech}}$ is the free energy density of the matrix. The purely incompressible result (*i.e.*, $K_{\mathtt{m}}\to\infty$) recovers the dilute estimate of Einstein (1906) and satisfies the well-known (Hashin and Shtrikman, 1963) bounds for such composites. Notably, the homogenization estimate in Eq. (12) holds for any I_1-based incompressible rigid-particle–matrix composite and was shown by Luo et al. (2023) to also be extremely accurate for quasi-incompressible matrices. Thus, the choice for the constitutive law of the matrix phase remains versatile in the present modeling framework. Evidently, in the limit of $c=0$, the homogenized energy recovers that of the matrix phase; *i.e.*, $\lim_{c\to 0}\Psi_{\mathtt{mech}}(I_1,J)=\Psi_{\mathtt{m,mech}}(I_1,J)$. By contrast, $\lim_{c\to 1}\Psi_{\mathtt{mech}}(I_1,J)=+\infty$, thus recovering the energy of a mechanically rigid material, such as that of the particle in the present case.

It is important to note that the above homogenized mechanical energy for the MRE may be replaced readily by any other mechanical energy of a phenomenological type that is available or better suited for the material at hand, as will be discussed in Section 5.

The magnetic energy. The magnetic free energy, $\rho_0\Psi_{\mathtt{mag}}$, in Eq. (11) reads (Mukherjee and Danas, 2022)

$$\rho_0\Psi_{\mathtt{mag}}(I_5^{\mathtt{B}},I_5^{\mathtt{BHr}},I_5^{\mathtt{Hr}})=-\frac{1}{2\mu_0}\frac{\chi^e}{1+\chi^e}I_5^{\mathtt{B}}+I_5^{\mathtt{BHr}}+\frac{\mu_0}{2}\left(\chi^e+\frac{1+2c}{3c}\right)I_5^{\mathtt{Hr}}+\frac{\mu_0}{c}\frac{(m^s)^2}{\chi_{\mathrm{p}}^r}f_{\mathrm{p}}\left(\frac{\sqrt{I_5^{\mathtt{Hr}}}}{m^s}\right). \tag{13}$$

In Eq. (13), χ_{p}^r is the *remanent susceptibility* of the underlying magnetic particles, whereas the "effective" parameters χ^e and m^s for the composite are given in terms of the particle magnetic properties and its volume fraction c as

$$\chi^e=\frac{3c\chi_{\mathrm{p}}^e}{3+(1-c)\chi_{\mathrm{p}}^e},\qquad \text{and}\qquad m^s=c\ m_{\mathrm{p}}^s\left(\frac{1+\chi_{\mathrm{p}}^e}{1+\chi^e}\right). \tag{14}$$

In this expression, χ_{p}^e and m_{p}^s are the particles' *energetic susceptibility* and *saturation magnetization*, respectively. To summarize, the energy in Eq. (13) involves a total of five magnetic parameters of the particles summarized in Table 1.

The saturation-type magnetization behavior of the *h*-MRE is captured by the nonlinear function $f_{\mathrm{p}}(x)$ in Eq. (13), whose choice needs to be made depending on the specific saturation response of the (hard/soft) magnetic particles. Representative examples of possible choices for the functional form of $f_{\mathrm{p}}(x)$ to describe different hard-magnetic particles have been provided in Mukherjee and Danas (2022) and Danas (2024) and are not repeated here for brevity. In what follows, we use the inverse hypergeometric function, which reads

$$f_{\mathrm{p}}(x)=-[\log(1-x)+x]. \tag{15}$$

The physical interpretation of the various parameters introduced above is elucidated using Fig. 2, which, for simplicity, refers to the case of $c=1$, corresponding to the magnetic response of pure particles (absent a matrix phase). Note that for *h*-MRE composites, which typically have $c\in(0,0.3]$ (Moreno et al., 2021), the interpretation we will provide remains qualitatively unchanged. Fig. 2a shows a schematic of a magnetic particle subjected to a full cyclic magnetic load $\mathbf{h}=h_1\mathbf{e}_1$. Given that the particle is considered mechanically rigid, in this plot we probe the purely magnetic laws described previously. In the plot of Fig. 2b, we observe that χ_{p}^e and χ_{p}^r combined together control the increasing slope of the magnetization curve past the coercive field b_{p}^c (to be discussed separately, below, in the context of the dissipation potential). In turn, χ_{p}^e alone controls the initial loading and unloading slope of the curve prior to reaching b_{p}^c or simply the relative magnetic permeability at zero magnetic loads and a pre-magnetized state. The parameter m_{p}^s defines the saturating value of the magnetization. The special case of $\chi_{\mathrm{p}}^e=0$ corresponds to an ideal magnet, *i.e.*, a magnet that reaches exactly the saturating m_{p}^s value at sufficiently large applied magnetic fields. By contrast, actual magnets continue to exhibit a slight increase of $\mathbf{m}$ up to large fields, a process that is controlled by the parameter χ_{p}^e, which typically has relatively small values ranging from 0.01 to 0.2.

The coupling energy. The proposed coupling free energy, $\rho_0\Psi_{\mathtt{couple}}$, in Eq. (11) is written as (Mukherjee and Danas, 2022)

$$\rho_0\Psi_{\mathtt{couple}}(I_4^{\mathtt{Hr}},I_5^{\mathtt{BHr}},I_5^{\mathtt{Hr}},I_6^{\mathtt{BHr}})=c\,\beta\left[\mu_0(1-2\chi^e)\left(I_4^{\mathtt{Hr}}-I_5^{\mathtt{Hr}}\right)-\frac{2\chi^e}{1+\chi^e}\left(I_6^{\mathtt{BHr}}-I_5^{\mathtt{BHr}}\right)\right]. \tag{16}$$

with the coupling parameter

$$\beta(c)=19c^2-10.4c+1.71,\qquad \forall c\in[0,0.3]. \tag{17}$$

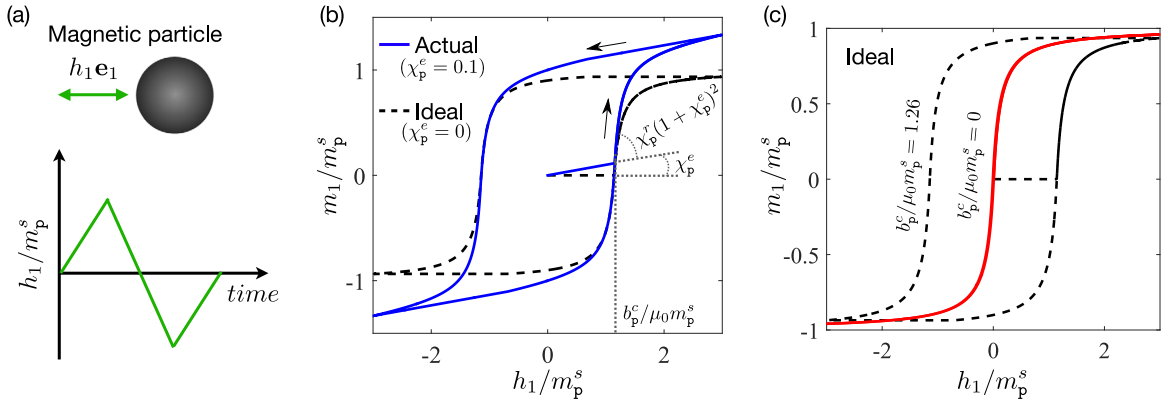

Fig. 2. (a) Schematic of a magnetic particle subjected to a full cyclic magnetic load $\mathbf{h} = h_1\mathbf{e}_1$. (b) Normalized magnetization response versus the normalized field strength. Both ideal ($\chi_\mathrm{p}^e = 0$; black dashed line) and actual ($\chi_\mathrm{p}^e = 0.1$; blue solid line) hysteresis loops are shown along with the slopes of the $m-h$ response before and after magnetic switching, *i.e.*, before and after reaching the value $b_\mathrm{p}^c/\mu_0 m_\mathrm{p}^s$. (c) Normalized magnetization responses for finite (black dashed line) and zero (red solid line) coercivity $b_\mathrm{p}^c/\mu_0 m_\mathrm{p}^s$ lead to, respectively, hysteretic and energetic magnetization responses.
Source: Both plots were adapted from the previous work of Mukherjee and Danas (2022).

The coefficients in this last equation were obtained by calibrating the analytical model to the corresponding 3D representative volume element (RVE) simulations of random distributions of magnetically hard particles in an elastomer matrix phase. This coupling parameter $\beta(c)$ may be independently calibrated against experimental data or other available numerical estimates if required. In Eq. (16), we highlight the simple linear dependence of the coupling energy density on the invariants, making it possible to obtain a dual energy density in the **F**-**H** space, as discussed in detail by Mukherjee and Danas (2022) and not shown here for brevity.

The dissipation potential. The dissipation potential D remains to be defined, which, along with the energy density W, will complete the constitutive relations in our model. Given that viscoelastic effects are not considered in the present manuscript (but see recent works in this direction by Rambausek and Danas (2021), Lucarini et al. (2022) and Stewart and Anand (2023)), the rate-independent dissipation potential is given in terms of $\dot{\mathcal{H}}^r$ only, such that (Mukherjee and Danas, 2019; Mukherjee et al., 2021a)

$$D(\dot{\mathcal{H}}^r) = b^c|\dot{\mathcal{H}}^r| \geq 0, \tag{18}$$

where $|.|$ denotes the standard Eulerian norm and b^c is the effective *coercive field* of the composite given by

$$b^c = b_\mathrm{p}^c\left(\frac{1+\chi^e}{1+\chi_\mathrm{p}^e}\right)^{4/5}. \tag{19}$$

In this expression, b_p^c and χ_p^e are the particle coercivity and energetic susceptibility, respectively, whereas χ^e has been defined in Eq. (14). Typically, for a hard-magnetic composite, the effective coercivity is given by $b^c = b_\mathrm{p}^c$ (Idiart et al., 2006). Nonetheless, the multiplicative term of b_p^c in Eq. (19) serves as an effective correction term for an actual magnet and can be obtained from available experimental data. From the plot in Fig. 2c, we observe that by letting $b_\mathrm{p}^c \to 0$ (and by extension $b^c \to 0$), one obtains a purely energetic magnetization response (without hysteresis), relevant for the modeling of *s*-MREs. This limit, however, is not analytical, and for this reason, alternative analytical expressions were proposed in Mukherjee et al. (2020) for the case of purely energetic *s*-MREs that are able to reproduce closely (Mukherjee and Danas, 2022; Danas, 2024) the limiting *s*-MRE response obtained by the present full dissipative model.

The derivative of the dissipation potential in Eq. (18) with respect to $\dot{\mathcal{H}}^r$ is non-unique at $|\dot{\mathcal{H}}^r| = 0$. Hence, we start from the Legendre–Fenchel transform of D, *i.e.*, D^*, such that

$$D^*(\mathcal{B}^r) = \inf_{\dot{\mathcal{H}}^r}\left[\mathcal{B}^r\cdot\dot{\mathcal{H}}^r - b^c|\dot{\mathcal{H}}^r|\right] \tag{20}$$

in the rate-independent limit. In this last expression, $\mathcal{B}^r$ is the remanent B-like field conjugate to $\dot{\mathcal{H}}^r$, such that upon the use of the condition in Eq. (20), one can define the dissipation potential also as $D = \mathcal{B}^r\cdot\dot{\mathcal{H}}^r \geq 0$. The minimization condition of the last expression leads to a criterion known as *ferromagnetic switching surface* (Landis, 2002; Mukherjee and Danas, 2019)

$$\Phi(\mathcal{B}^r) := |\mathcal{B}^r|^2 - (b^c)^2 = 0, \tag{21}$$

which must be satisfied during the energy dissipation in a magnetic loading/unloading cycle. With Eq. (21), one may recast the dissipation potential $D(\dot{\mathcal{H}}^r)$ by introducing a (non-negative) Lagrange multiplier $\dot{\Lambda}$, so that

$$D(\dot{\mathcal{H}}^r) = \sup_{\mathcal{B}^r}\ \inf_{\dot{\Lambda}\geq 0}\left[\mathcal{B}^r\cdot\dot{\mathcal{H}}^r - \dot{\Lambda}\Phi(\mathcal{B}^r)\right]. \tag{22}$$

In fact, substituting $\mathcal{B}^r = b^c\dot{\mathcal{H}}^r/|\dot{\mathcal{H}}^r|$ (the minimization condition of Eq. (20)) yields exactly $D(\dot{\mathcal{H}}^r) = b^c|\dot{\mathcal{H}}^r|$ but now with the constraint in Eq. (21), which must be satisfied to make the term $\dot{\Lambda}\Phi(\mathcal{B}^r)$ in Eq. (22) vanish.

The constrained dissipation potential in Eq. (22) leads to the following set of equations necessary to obtain the evolution of $\boldsymbol{\mathcal{B}}^r$:

$$\dot{\boldsymbol{\mathcal{H}}}^r = \dot{\lambda}\frac{\partial \boldsymbol{\Phi}}{\partial \boldsymbol{\mathcal{B}}^r}, \qquad \boldsymbol{\Phi}(\boldsymbol{\mathcal{B}}^r) \le 0, \qquad \dot{\lambda} \ge 0 \qquad \text{and} \qquad \dot{\lambda}\boldsymbol{\Phi} = 0, \tag{23}$$

with $\boldsymbol{\mathcal{H}}^r(t=0) = \mathbf{0}$. These conditions are also known as the Karush–Kuhn–Tucker (KKT) conditions (Karush, 1939; Kuhn and Tucker, 1951).

With Eq. (23), the evolution equations for the internal vector variable $\boldsymbol{\mathcal{H}}^r$ are now fully defined, concluding our overview of the fully dissipative h-MRE model of Mukherjee et al. (2021a) and Mukherjee and Danas (2022). Evidently, this model is path- and history-dependent. Its mathematical similarity to J_2 flow theory of plasticity allows us to resort to already well-known numerical algorithms (such as the radial return algorithm) to resolve the evolution equations and evaluate the deformation and magnetic fields under general magneto-mechanical loads. The model must be solved numerically, as is the case in all incremental elasto-plastic models in the literature. Yet, our model for MREs is explicit in the sense that all expressions are analytical and, thus, straightforward to implement in material subroutines to solve general boundary value problems (Rambausek et al., 2022). Numerical implementations of the model in user element routines for Abaqus and FEniCS are available in Mukherjee et al. (2021b) and Rambausek et al. (2021). Corresponding predictions of the proposed model may also be found in those papers and are not repeated here for conciseness.

In closing this section, it is worth noting that it is possible to further enrich the present modeling framework to take into account more complex magnetic phenomena if deemed necessary. Possible areas for extension include switching surface shrinking during asymmetric cyclic loads, the evolution of the coercivity with temperature, or even rate or frequency effects. However, at present, there is a striking lack of experiments in the literature to study these phenomena. These experiments must be tackled first so that their results can inform future model extensions. A first effort towards this direction may be found in the earlier work of Mukherjee and Danas (2019).

4. An energetic model for small magnetic fields after pre-magnetization

For small amplitudes of the applied magnetic field, where the norm of the remanent $\boldsymbol{\mathcal{B}}^r$ field is smaller than the coercive value b_p^c, or simply, when $\boldsymbol{\Phi} < 0$ in Eq. (21), $\boldsymbol{\mathcal{H}}^r$ remains constant (in time) throughout the actuation process even when the applied deformation is large. This observation enables us to propose a simplified purely energetic model obtained from the more general dissipation model discussed in Section 3. To do so, we set a constant amplitude and direction to $\boldsymbol{\mathcal{H}}^r$ (Moreno-Mateos et al., 2022b, 2023)

$$\boldsymbol{\mathcal{H}}^r = \boldsymbol{C}, \quad |\boldsymbol{C}| < Q \tag{24}$$

with Q denoting some real non-infinite number. Since $\boldsymbol{\mathcal{H}}^r$ is constant,[4] variations of the energy with respect to $\boldsymbol{\mathcal{H}}^r$ are null and one may write a purely energetic model defined by the energy density

$$W^{\mathrm{e}}(\mathbf{F}, \mathbf{B}; \boldsymbol{\mathcal{H}}^r) = \rho_0 \Psi_{\mathtt{mech}}(I_1, J) + \rho_0 \Psi_{\mathtt{mag}}(I_5^{\mathrm{B}}, I_5^{\mathrm{BHr}}) + \rho_0 \Psi_{\mathtt{couple}}(I_4^{\mathrm{Hr}}, I_5^{\mathrm{BHr}}, I_6^{\mathrm{BHr}}) + \frac{1}{2\mu_0 J} I_5^{\mathrm{B}}, \tag{25}$$

where the superscript e stands for "energetic".

In this last definition, naturally, the mechanical energy density term remains unchanged from Eq. (12).

The purely magnetic free energy written in Eq. (13) now simplifies to

$$\rho_0 \Psi_{\mathtt{mag}}(I_5^{\mathrm{B}}, I_5^{\mathrm{BHr}}) = -\frac{1}{2\mu_0 J}\frac{\chi^e}{1+\chi^e} I_5^{\mathrm{B}} + I_5^{\mathrm{BHr}}, \tag{26}$$

with χ^e given by Eq. (14). Furthermore, any terms in the energy that only involve $\boldsymbol{\mathcal{H}}^r$ (but no $\mathbf{F}$ or $\mathbf{B}$) are constant and, thus, can be dropped. For this case of small magnetic loading, the coupled energy term is obtained by simplifying the original coupling energy density written in Eq. (16) to

$$\rho_0 \Psi_{\mathtt{couple}}(I_4^{\mathrm{Hr}}, I_5^{\mathrm{BHr}}, I_6^{\mathrm{BHr}}) = c\beta(c)\left[\mu_0(1-2\chi^e) I_4^{\mathrm{Hr}} - \frac{2\chi^e}{1+\chi^e}\left(I_6^{\mathrm{BHr}} - I_5^{\mathrm{BHr}}\right)\right]. \tag{27}$$

Remark 3. Both the amplitude and direction of the internal variable $\boldsymbol{\mathcal{H}}^r$ need to be prescribed in this simplified energetic model. They can be proposed heuristically based on intuitive arguments (as is usually done in the literature for simple structures). Alternatively, they need to be evaluated from an independent calculation of the magnetic dissipation to estimate the pre-magnetization profile in a magnetoelastic structure (Mukherjee and Danas, 2022).

Current magnetization. Using the above expressions, one may directly evaluate the current magnetization in the h-MRE. Noting from the polar decomposition in (1) that $\mathbf{F}^{-T} = \mathbf{R}\,\mathbf{U}^{-1}$ and $\mathbb{C}^{1/2} = \mathbf{U}$ (since $\mathbb{C} = \mathbf{U}^2$), one can show using Eq. $(3)_2$ that

[4] We precise here that $\boldsymbol{\mathcal{H}}^r$ may vary in space, i.e., along the length of a beam but does not change with the applied loads in time.

$$\mathbf{h} = \mathbf{F}^{-T}\mathbf{H} = \mathbf{F}^{-T}\frac{\partial W^{\mathrm{e}}}{\partial \mathbf{B}} = \frac{1}{\mu_0 J}\mathbf{F}\,\mathbf{B} - \frac{\chi^e}{\mu_0 J(1+\chi^e)}\mathbf{F}\,\mathbf{B} + \mathbf{R}\boldsymbol{\mathcal{H}}^r + \frac{2c\beta\chi^e}{1+\chi^e}(\mathbf{R}\,\boldsymbol{\mathcal{H}}^r - \mathbf{R}\,\mathbb{C}\,\boldsymbol{\mathcal{H}}^r). \tag{28}$$

Next, use of Eq. $(3)_1$ leads to

$$\mathbf{h} = \frac{1}{\mu_0}\mathbf{b} - \frac{\chi^e}{\mu_0(1+\chi^e)}\mathbf{b} + \mathbf{R}\boldsymbol{\mathcal{H}}^r + c\beta\frac{2\chi^e}{1+\chi^e}(\mathbf{R}\,\boldsymbol{\mathcal{H}}^r - \mathbf{R}\,\mathbb{C}\,\boldsymbol{\mathcal{H}}^r). \tag{29}$$

A direct comparison between this last relation and the definition for the current magnetization in Eq. (2) yields

$$\mathbf{m} = \frac{\chi^e}{\mu_0(1+\chi^e)}\mathbf{b} - \mathbf{R}\boldsymbol{\mathcal{H}}^r - \frac{2c\,\beta\,\chi^e}{1+\chi^e}(\mathbf{R}\,\boldsymbol{\mathcal{H}}^r - \mathbf{R}\,\mathbb{C}\,\boldsymbol{\mathcal{H}}^r), \tag{30}$$

which provides a relation between $\mathbf{m}$, $\mathbf{b}$, and $\boldsymbol{\mathcal{H}}^r$ in the energetic, coupled model proposed here.

Certain observations follow:

- In the absence of an applied magnetic field $\mathbf{b}$, the current magnetization $\mathbf{m}$ is only a function of $\boldsymbol{\mathcal{H}}^r$ and the rotation part of the deformation gradient $\mathbf{R}$.
- In the case of non-ideal h-MRE, where $\chi^e \neq 0$ (see the example in Fig. 2 or Stepanov et al. (2017) and Mukherjee and Danas (2019) for relevant experimental data), $\mathbf{m}$ evolves with the (applied) Eulerian magnetic flux $\mathbf{b}$ (as shown in Fig. 2b) with a slope that is not μ_0 but depends on χ^e. In turn, χ^e is a function of the particle permeability and volume fraction as defined in Eq. (14). Note, however, that in realistic h-MREs, χ^e is rather small (*i.e.*, $\chi^e \sim 0.01 - 0.2$) and, thus, may be neglected in several cases of interest (Zhao et al., 2019).
- We observe that $\mathbf{m}$ is not a proper internal variable since, still in the general case of non-ideal h-MREs, $\mathbf{m}$ depends also on $\mathbf{b}$ and not only on $\boldsymbol{\mathcal{H}}^r$.
- The last term in Eq. (30) implies that for non-ideal magnets with $\chi^e \neq 0$, $\mathbf{m}$ will change with the application of a stretch in the full energetic model defined in Eq. (25). Nevertheless, this last term is substantially smaller than the first two, since in actual h-MREs, $\chi^e \sim 0.01 - 0.2$ and $c\beta$ are of a similar order when $c \leq 0.3$. This implies that this term is, in practice, very small and will essentially lead to negligible changes in magnetization amplitude for stretches as large as three (*i.e.*, 200% strain). As such, we reiterate the observation that $\mathbf{m}$ is a function of $\boldsymbol{\mathcal{H}}^r$ and *nearly* stretch independent in most cases of practical interest. This term, however, derives from the coupling part of the energy, which is essential for the prediction of magnetostriction at large magnetic fields.

4.1. Special case of uncoupled, ideal h-MRE

The case of an ideal magnetic (energetic) h-MRE, i.e., one with ideal magnetic particles (see Fig. 2b) has been extensively used in the literature owing mainly to the seminal work of Zhao et al. (2019), which focuses, however, on slender MRE structures subjected mainly to bending deformations. Next, we provide a detailed discussion of how the full energetic model in Eq. (25) can be simplified for the case of ideal magnetic h-MREs and comment on the implications of this simplification.

We start by using an uncoupled magneto-mechanical energy, an approximation that was considered in the earlier models of Zhao et al. (2019) and Yan et al. (2023), as well as more recently in Moreno-Mateos et al. (2023), and can be implemented by setting $\beta = 0$ in Eq. (27), leading to

$$\rho_0\Psi_{\mathtt{couple}} = 0. \tag{31}$$

Here, the notion of an uncoupled response is meant in the sense of the homogenization analysis carried out by Danas (2017), where it was shown that under the application of a Eulerian magnetic field $\mathbf{b}^{\mathtt{app}}$, the purely magnetic energy in Eq. (26) induces no net intrinsic magnetostriction of the MRE. Nonetheless, by *uncoupled*, one should not be confused with the apparent magneto-mechanical coupling induced between a magnetic structure (even with negligible magnetostriction) and the surrounding magnetic field; this is, in fact, a strong effect with the rotation of a metallic needle in a compass the canonical example. While the compass needle has negligible magnetostrictive strains, the structure interacts with the surrounding magnetic field to indicate the direction of the Earth's magnetic poles.

Another approximation required to recover the magnetic response of an ideal h-MRE consists in setting $\chi^e_{\mathrm{p}} = 0$, and thus $\chi^e = 0$, in the energetic model of Eq. (25). This approximation simplifies the magnetic energy in Eq. (26) to

$$\rho_0\Psi_{\mathtt{mag}}(I_5^{\mathtt{BHr}}) = I_5^{\mathtt{BHr}} = \mathbf{B}\cdot\mathbb{C}^{1/2}\boldsymbol{\mathcal{H}}^r. \tag{32}$$

The effect of setting $\chi^e_{\mathrm{p}} = 0$ has been discussed in Section 3.3 (cf. Fig. 2b) and serves to impose that the relative magnetic permeability of a pre-magnetized h-MRE is exactly equal to unity in the absence of an applied magnetic field.

Gathering the approximations and statements provided above, we obtain the following simplified energetic model for an ideal h-MRE:

$$\begin{aligned} W^{\mathrm{e,R}}(\mathbf{F},\mathbf{B};\boldsymbol{\mathcal{H}}^r) &= \rho_0\Psi_{\mathtt{mech}}(I_1,J) + I_5^{\mathtt{BHr}} + \frac{1}{2\mu_0 J}I_5^{\mathrm{B}} \\ &= \rho_0\Psi_{\mathtt{mech}}(I_1,J) + \mathbf{B}\cdot\mathbb{C}^{1/2}\boldsymbol{\mathcal{H}}^r + \frac{1}{2\mu_0 J}\mathbf{B}\cdot\mathbb{C}\,\mathbf{B}. \end{aligned} \tag{33}$$

Following the same steps presented in Eq. (28), or simply setting $\chi^e = 0$ in Eq. (30), one can readily show that in the present case of an uncoupled, ideal h-MRE, the current magnetization is

$$\mathbf{m} = -\mathbf{R}\boldsymbol{\mathcal{H}}^r. \tag{34}$$

Importantly, given the starting assumptions, especially in light of Eq. (24), we observe that the magnitude of the current magnetization, $|\mathbf{m}| = |\boldsymbol{\mathcal{H}}^r| = |\mathbf{h}^r|$, remains unchanged with the application of a small applied (external) magnetic field and is entirely stretch-independent. Even in this simplified case, $\mathbf{m}$ cannot formally serve as an internal variable since it depends on the rotation $\mathbf{R}(\mathbf{F})$, which itself is a function of the deformation gradient. By contrast, it is evident that $\mathbf{m}$ will exhibit properties similar to $\boldsymbol{\mathcal{H}}^r$, which, by definition, is an internal variable (and independent of $\mathbf{F}$ or $\mathbf{B}$).

For the purpose of comparing this uncoupled model with the models of Yan et al. (2023) (cf. Section 5) and Zhao et al. (2019) (cf. Section 6), it is helpful to define an energy per unit current volume $w^{\mathrm{e,R}} = W^{\mathrm{e,R}}/J$, which, together with the result Eq. (34), reads

$$W^{\mathrm{e,R}}(\mathbf{F}, \mathbf{b}, \boldsymbol{\mathcal{H}}^r) = \rho_0 \Psi_{\mathtt{mech}}(I_1, J) + J\, \mathbf{R}\boldsymbol{\mathcal{H}}^r \cdot \mathbf{b} + \frac{J}{2\mu_0}\mathbf{b}\cdot\mathbf{b}, \tag{35}$$

or equivalently

$$w^{\mathrm{e,R}}(\mathbf{F}, \mathbf{b}, \boldsymbol{\mathcal{H}}^r) = \frac{\rho_0}{J}\Psi_{\mathtt{mech}}(I_1, J) - \mathbf{m}\cdot\mathbf{b} + \frac{1}{2\mu_0}\mathbf{b}\cdot\mathbf{b}. \tag{36}$$

It is straightforward to show then that

$$\frac{\partial w^{\mathrm{e,R}}}{\partial \mathbf{b}} = -\mathbf{m} + \frac{1}{\mu_0}\mathbf{b} = \mathbf{h}. \tag{37}$$

Remark 4. The derivatives of both the coupled, W^{e}, and the uncoupled $W^{\mathrm{e,R}}$ energies with respect to $\mathbf{F}$ lead to a symmetric total Cauchy stress, which may be split to a sum of an energetic mechanical stress and a Maxwell stress. Those expressions have been discussed extensively in Mukherjee and Danas (2022) and are not reported here for brevity.

5. The energetic model of Yan et al. (2023)

Following an approach similar to that of Zhao et al. (2019) and Yan et al. (2023) proposed a magneto-elastic model for h-MREs valid for small magnetic fields around a pre-magnetized state. Inspired by their own experimental results, the model in Yan et al. (2023) does, however, take into consideration the stretch-independency of $\mathbf{m}$, contrary to that of Zhao et al. (2019), which does not.

To facilitate the comparison between these existing models and the framework presented in this work, we have updated their notation in the summary of the model of Yan et al. (2023) provided next. The behavior of a bulk, magnetically ideal h-MRE under a small applied magnetic field and a fully pre-magnetized state is described by a Helmholtz free energy density, summing an elastic mechanical part, $\rho_0\Psi_{\mathtt{mech}}$ and a magnetic part, $\rho_0\Psi^{\mathtt{RM}}_{\mathtt{mag}}$, [5] such that

$$w^{\mathtt{RM}}(\mathbb{C}, \mathbf{b}, \mathbf{m}) = \frac{\rho_0}{J}\Psi_{\mathtt{mech}}(I_1, J) + \frac{\rho_0}{J}\Psi^{\mathtt{RM}}_{\mathtt{mag}}(\mathbf{m}, \mathbf{b}). \tag{38}$$

For the mechanical part, the authors used a simple quasi-incompressible neo-Hookean model of the form

$$\frac{\rho_0}{J}\Psi^{\mathtt{RM}}_{\mathtt{mech}}(I_1) = \frac{G}{2}(J^{-2/3}\mathbf{F}^T\cdot\mathbf{F} - 3) + \frac{K}{2}(J-1)^2. \tag{39}$$

In this expression, the shear, G, and bulk, K, moduli of the h-MRE may be either measured directly from experiments or estimated using the homogenization result in Eq. (12). For the experimentally relevant case of a neo-Hookean matrix phase and mechanically rigid particles, use of the homogenization estimates leads to (Lopez-Pamies et al., 2013; Luo et al., 2023)

$$G = \frac{G_{\mathtt{m}}}{(1-c)^{\frac{5}{2}}}, \quad \text{and} \quad K = \frac{K_{\mathtt{m}}}{2(1-c)^6}, \tag{40}$$

where $G_{\mathtt{m}}$ is the shear modulus of the polymer matrix and c is the volume fraction of the rigid NdFeB particles.

The corresponding magnetic energy reads

$$\frac{\rho_0}{J}\Psi^{\mathtt{RM}}_{\mathtt{mag}}(\mathbf{m}, \mathbf{b}) = -\mathbf{m}\cdot\mathbf{b}. \tag{41}$$

Subsequently, the authors, making use of direct experimental evidence and numerical results of Mukherjee et al. (2021a), described the pre-magnetized state using a magnetization measure $\mathbf{M}$, which is *constitutively* linked to the current magnetization $\mathbf{m}$ via

$$\mathbf{m} = J^{-1}\mathbf{R}\mathbf{M}, \qquad \mathbf{M} \in \mathbb{R}^3. \tag{42}$$

[5] In the original studies of (Yan et al., 2023, 2021), the notation $U^{\mathrm{e}} \equiv \rho_0\Psi_{\mathtt{mech}}$ and $U^{\mathtt{m}} \equiv \rho_0\Psi^{\mathtt{RM}}_{\mathtt{mag}}$ was used.

The vector $\mathbf{M}$ serves to describe the pre-magnetization state, which remains fixed during actuation. More importantly, the fact that $\mathbf{M}$ is related to the current $\mathbf{m}$ via $\mathbf{R}$ (and not via $\mathbf{F}$) implies that it lies at an intermediate stretch-free configuration. By direct comparison with the energetic models presented in Section 4.1, one can connect the internal variable $\boldsymbol{\mathcal{H}}^r$ and $\mathbf{M}$ simply by setting

$$\boldsymbol{\mathcal{H}}^r = -J^{-1}\mathbf{M}. \tag{43}$$

As such, the model of Yan et al. (2023) turns out be exactly equivalent (up to the background term $1/\mu_0\mathbf{b}\cdot\mathbf{b}$) to the simplified, energetic version of the Mukherjee et al. (2021a) and Mukherjee and Danas (2022) model presented in Eq. (36).

6. The Zhao et al. (2019) model versus the energetic models of Mukherjee et al. (2021a) and Yan et al. (2023)

In the original work of Zhao et al. (2019), the authors considered a remanent magnetic field,[6] $\mathbf{b}^r$, which has the characteristics of an internal variable similar to $\boldsymbol{\mathcal{H}}^r$ defined in Eq. (8). They also assumed that $\mathbf{b}$ and $\mathbf{h}$ remain linear and with a slope μ_0 at small applied fields (*i.e.*, ideal h-MREs), which is a fair assumption since the relative permeability in such materials is close to unity, as already discussed in Section 1. Together with the very definition of the current magnetization in Eq. (2), this assumption yields

$$\mathbf{h} = \frac{1}{\mu_0}(\mathbf{b}-\mathbf{b}^r) \qquad \Rightarrow \qquad \mathbf{b}^r = \mu_0\mathbf{m}. \tag{44}$$

Subsequently the field $\mathbf{b}^r$ is pulled back to obtain a Lagrangian remanent field, $\mathbf{B}^r$ (denoted as $\tilde{\mathbf{B}}^r$ in their article), defined as

$$\mathbf{B}^r = J\mathbf{F}^{-1}\mathbf{b}^r = J\mu_0\mathbf{F}^{-1}\mathbf{m}, \tag{45}$$

which is directly related to the remanent field in the h-MRE after strong pre-magnetization. By contrast, during pre-magnetization the above relation implies

$$\frac{1}{J}\mathbf{F}\mathbf{B}^r = \mathbf{b}^r = \mu_0\mathbf{M}, \tag{46}$$

and leads to $\mathbf{h}=\mathbf{0}$ during the pre-magnetization operation.

Subsequently, $\mathbf{B}^r$ is chosen as the main independent state variable in the problem, leading to the following definition of the energy density:

$$w^{\mathrm{FM}}(\mathbb{C},\mathbf{b},\mathbf{m}) = \frac{\rho_0}{J}\Psi_{\mathtt{mech}}(I_1,J) - \frac{1}{J\mu_0}\mathbf{F}\mathbf{B}^r\cdot\mathbf{b}. \tag{47}$$

Importantly, this form of the energy density implies that the constant Lagrangian remanent field,[7] $\mathbf{B}^r$, directly leads to strong stretch-dependent $\mathbf{b}^r$ and $\mathbf{m}$. As a consequence, it follows that for arbitrary stretches $\mathbf{U}$ (from the polar decomposition $\mathbf{U}=\mathbf{R}^T\mathbf{F}$), their model predicts that the current magnetization could become substantially larger than the saturation magnetization of the h-MRE since it evolves with the deformation gradient $\mathbf{F}$.

By contrast, Zhao et al. (2019) have only implemented and used the proposed $\mathbf{F}$-$\mathbf{B}^r \equiv \mathbf{F}$-$\mathbf{M}$ model in situations of very small stretches, such as bending of an actuated beam or plate, which are both slender geometrically and thus use of the inextensibility condition results naturally to a stretch independent magnetization response. If, however, the plate, shell or beam is stretched, as is the case in the experimental results of Yan et al. (2023) and the recent studies of Stewart and Anand (2023) and Zhang et al. (2023), then significant discrepancies may be observed between the **FM** model of Zhao et al. (2019) and the **RM** model of Yan et al. (2023) and that of Mukherjee et al. (2021a).

We proceed by reviewing the subset of results from Yan et al. (2023) that are relevant to, and provide evidence for, the discussion in the paragraph above. For convenience, these results are reproduced in Fig. 3. As shown in the schematic diagram of Fig. 3a, their system comprised a square-shaped, thin, h-MRE plate (side length $L = 25$ mm and thickness $h = 505$ μm) that was clamped on all of its 4 sides. The plate was magnetized along $\mathbf{e}_3 = \mathbf{M}/|\mathbf{M}|$, which is also the direction of the applied magnetic field $\mathbf{b}^{\mathrm{app}}$. A pneumatic chamber induces an internal pressure p. The deflection of the plate along $\mathbf{e}_3$ is quantified by the maximum value, δ, at its center. We point the reader to the original manuscript of Yan et al. (2023) for additional details (*e.g.*, fabrication, additional physical properties, and experimental protocol). In Fig. 3b,c, we reproduce their experimental data (closed symbols) for the measured normalized deflection, δ/h as a function of the applied pressure, p, for two values of the amplitude of the applied magnetic field, $|\mathbf{b}| = \{80, 160\}$ mT. At the same value of the applied pressure p, a higher magnetic field resists the plate deflection. The corresponding 3D FEM results (open symbols) are presented in Fig. 3b using the **RM** model and in Fig. 3c using the **FM** model. The authors found that the **RM** model provides predictions in excellent agreement with the experimental data, whereas the **FM** model does not. The pneumatic loading induces non-negligible stretching deformation of the plate's mid-surface, calling for an appropriate description of the magnetization of the deformed plate according to Eq. (42) (**RM** model) and that the **FM** model by Zhao et al. (2019) is inappropriate in this case. Note that Yan et al. (2023), as well as other studies mentioned in Section 1, also investigated several other cases of slender structures that effectively behaved as inextensible, for which the predictions from the **FM** model were satisfactory.

[6] The remanent magnetic field was denoted as $\mathbf{B}^r$ in their article.

[7] The Lagrangian remanent field, $\mathbf{B}^r$, may be identified with the pre-magnetized state by setting $\mathbf{B}^r = \mu_0\mathbf{M}$ in the notation of Yan et al. (2023).

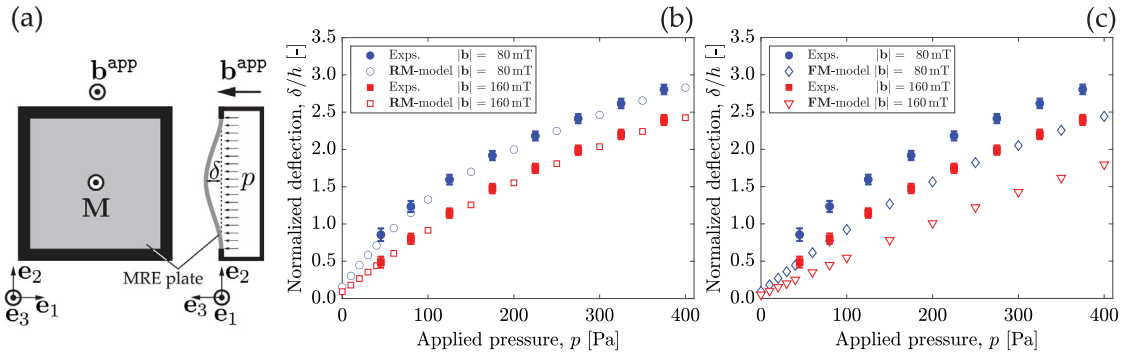

Fig. 3. Results reproduced from Yan et al. (2023) for experiments and FEM simulations, the latter for both the **RM** and the **FM** models, for a fully clamped h-MRE plate under combined pressure and magnetic loading. (a) Schematic diagram with a top view (into the $\mathbf{e}_1$-$\mathbf{e}_2$ plane) and side view (into the $\mathbf{e}_2$-$\mathbf{e}_3$ plane) of the system. (b,c) Normalized deflection, δ/h versus the applied pressure p, for two values of the amplitude of the applied magnetic field, $|\mathbf{b}| = \{80, 160\}$ mT. The experimental results (solid symbols) are common to both plots. (b) Comparison between the experimental results and 3D FEM-simulations (open symbols) using the **RM** model: circles and squares for 80 mT and 160 mT, respectively. (c) Comparison between the experimental results and 3D FEM-simulations (open symbols) using the **FM** model: open diamonds and triangles for 80 mT and 160 mT, respectively.
Source: This figure was adapted from the previous work of Yan et al. (2023).

7. Discussion and limitations of the simplified models

We proceed by commenting on the fact that the models of Zhao et al. (2019) and Yan et al. (2023) and many others thereafter in the literature neglect the background energy term $\mathbf{B}\cdot\mathbb{C}\,\mathbf{B}/2\mu_0 J$; cf. the last term in Eq. (36). One may directly add this term in Eqs. (38) and (47), similar to the energy definitions in Eqs. (25), (36), and (35). However, in that case, $\mathbf{B}$ (or $\mathbf{b}$) becomes an unknown field with prescribed boundary conditions and needs to be solved for, together with the displacement field. Instead, dropping this background magnetic term may be justifiable, but *only* under specific conditions, which are summarized as follows[8]:

i. the externally applied magnetic field is spatially uniform (*i.e.*, it is applied far from the specimen),
ii. the MRE geometry is such that the $\mathbf{B}$ and $\mathbf{H}$ fields are (or may be approximated to be) uniform in the specimen,
iii. the Eulerian magnetic flux $\mathbf{b}$ or magnetic strength $\mathbf{h}$ in the specimen can be assumed to be equal to the externally applied Eulerian magnetic flux $\mathbf{b}^{\text{app}}$ or $\mathbf{h}^{\text{app}}$, respectively,
iv. the Eulerian magnetic strength $\mathbf{h}$ or magnetic flux $\mathbf{b}$ during pre-magnetization are approximately zero (for applied $\mathbf{b}^{\text{app}}$ or $\mathbf{h}^{\text{app}}$, respectively), such that relation in Eq. (46) holds.

In the specific situations stated above, due to the normal continuity of $\mathbf{B}$ and the tangential continuity of $\mathbf{H}$, it can be readily shown that the leading order tractions due to Maxwell stresses resulting from the background magnetic energy term, $\mathbf{B}\cdot\mathbb{C}\,\mathbf{B}/2\mu_0 J$, inside the MRE and the surrounding air are identically equilibrated. As such, this term has no net impact on the *mechanical* response of the MRE (soft or hard), and the torque exerted upon the structure via the magnetic field is $\mathbf{b}^{\text{app}}\times(\mu_0\mathbf{M})$. Note that, in actual experimentally relevant situations, this assumption may introduce errors, which can be negligible or substantial, depending on the geometry of the device and/or the MRE. Certain important counter-examples of practical relevance are discussed next.

Near corners of the MRE structure, the magnetic fields cannot be uniform by standard physical arguments (*e.g.*, the requirement of a divergence-free $\mathbf{B}$ and a curl-free $\mathbf{H}$), also known as Fringe effects. In bulk specimens, it was shown for small strains by Brown (1966), and for finite strains by Lefèvre et al. (2017), that the mechanical and magnetic fields are not uniform inside an MRE specimen, even when the far-applied pre-magnetization or actuation magnetic field is uniform. This non-uniformity becomes less pronounced in slender structures except near the edges of the specimen.

Another case where assumptions (iii) and (iv) are not satisfied occurs when a uniformly pre-magnetized (along the long axis) h-MRE beam is at an angle with respect to the applied actuation magnetic field. In this configuration, the magnetic flux in the solid cannot be the same as that of the external air since a non-zero component exists along the beam's long axis. At one hand, this component will affect the shear strains and stresses in the beam. On the other hand, this component is not expected to affect strongly the overall deflection of the beam at the initial stages of deformation if the main deformation mode is pure bending. Yet, this non-zero component of the resulting magnetic flux during actuation along the beam's long axis may strongly affect the response of the system at large applied fields and more complex structures or more complex pre-magnetization profiles (Mukherjee and Danas, 2022).

Another example where the background magnetic energy cannot be neglected can be found in the work of Psarra et al. (2019) studying a system comprising a thin s-MRE film attached to a passive elastic substrate. Their experimental and numerical investigation clearly showed that the shear stresses in the film lead to a crinkling instability pattern with pronounced angular

[8] See also the related discussion in Sharma and Saxena (2020).

out-of-plane protrusions similar to the ferrofluid Rosensweig instability (Cowley and Rosensweig, 1967). In that study, the proper resolution of the surrounding magnetic energy and the interaction between neighboring wrinkles/crinkles turned out to be of critical importance to correctly capture the experimentally observed deformation pattern.

Similarly, condition (iv) in the above list can only be valid when the pre-magnetization field has a simple uniform distribution along the principal directions of the slender structure. When, for instance, the pre-magnetization is conducted on pre-curved slender structures (Ren et al., 2019), despite being slender, both $\mathbf{b}$ and $\mathbf{h}$ fields are non-null and thus neither of them can be directly and analytically identified with the external applied magnetic fields. Furthermore, in those cases, the pre-magnetized state does not correlate directly with the pre-deformed shape of the structure (Mukherjee and Danas, 2022), and thus, a full simulation of the boundary value problem (BVP) is required to estimate the actual pre-magnetization state.

In actual magnetic setups, the applied pre-magnetization or actuating magnetic fields may be non-uniform (Dorn et al., 2021). A rather critical assessment of several popular setups and their influence on the MRE response has been recently carried out in Moreno-Mateos et al. (2023). In such cases, none of the above conditions holds true, calling for simulations of the full BVP. Yan et al. (2021) and Sano et al. (2022a) have also addressed the general case of non-uniform fields with a constant gradient (albeit using the previous **FM** model only valid for negligible stretching) by incorporating the magnetic body force induced by the field gradient and implementing it in FE packages. Yan et al. (2021) focused on the planar (2D) deformation of geometrically nonlinear hard-magnetic beams, whereas (Sano et al., 2022a) studied the 3D deformation of hard-magnetic rods following a Kirchhoff rod theory framework. Given the slenderness of these beams and rods, the specific loading conditions, and the relatively small magnitude of the applied actuating magnetic fields, both of these systems remained effectively inextensible. As such, it was appropriate for the authors to employ the **FM** model, in lieu of the **RM** one, and also without a need to consider the $\Psi_{\texttt{couple}}$ term in the energy density of Eq. (25).

For more complex and multi-component h-MRE structures, which may exhibit self-interactions, one should take into account the surrounding air in the modeling approach. The chosen approach may vary depending on the BVP at hand, the complexity of the geometry, and the convergence properties of the numerical scheme. We point the interested reader to a number of recent efforts along this direction: the staggered approach (Pelteret et al., 2016) (see also Rambausek et al. (2022) for improvements), the penalty method of constraining the air–solid boundary node sets (Psarra et al., 2017, 2019), and the more straightforward use of a very soft mechanical law for the air (see for instance (Dorn et al., 2021) and improvements in Rambausek et al. (2022) and Moreno-Mateos et al. (2022a)). More recently, a non-local approach coupling interacting faces in a beam structure by use of dipole–dipole interactions has been proposed by Sano (2022b) to rationalize previously unexplained experimental observations in Sano et al. (2022a). Finally, two additional promising approaches, not discussed here, have been proposed in Rambausek and Schöberl (2023), where a proper treatment of the Maxwell stress at the interface between the magnetoelastic solid and the air allows to eliminate the spurious modes present in such problems and allow for good convergence.

Finally, and from a more mathematical point of view, we note that the omission of the background magnetic energy may lead to non-symmetric stress measures and incomplete descriptions of the magnetic constitutive relations. For instance, we observe that neglecting the term $\mathbf{b}\cdot\mathbf{b}/2\mu_0$ in Eq. (36) would lead to an incomplete definition for the magnetic field strength in Eq. (37); *i.e.*, $\partial w^{\mathrm{e,R}}/\partial\mathbf{b} = -\mathbf{m}$ and not $\mathbf{h}$. Dorfmann and Ogden (2024) recently made a similar observation in their work on energy considerations and energetic magnetization models for h-MREs, further supporting the notion that magnetization alone is insufficient to fully describe a magneto-mechanical problem.

8. Conclusion

In this study, we aimed to elucidate several crucial aspects concerning the modeling of h-MREs (but also potentially relevant for a large set of particle-filled s-MREs) and, in particular, the stretch-independence of their magnetization response, which has been observed experimentally and numerically. Such a property needs to be taken into account appropriately in the modeling so as to avoid inaccurate or nonphysical predictions (*e.g.*, a magnetization that is larger than the magnetization saturation of the MRE) that may result when the tested MRE is subjected to pre-stretching or pre-stressing. We have shown that the fully dissipative model of Mukherjee et al. (2021a) may be reduced, under certain physically sound assumptions, to the energetic model of Yan et al. (2023), but not that of Zhao et al. (2019). The former two models were shown to be in agreement with experiments on slender structures. Furthermore, the more complete dissipative model of Mukherjee et al. (2021a) was also shown to be in very good agreement with full-field numerical simulations of representative volume elements of h-MREs subjected to finite stretching and magnetic fields and not only pure bending.

As an additional outcome of the present analysis, we have shown that the magnetization has the properties of an internal variable, and as such, it is subject to constitutive assumptions. Specifically, the use of a direct pull-back or push-forward of the current magnetization may lead to incorrect predictions that are inconsistent with experimental measurements or full-field simulations. The reason lies in the fact that in a finite strain formulation, the magnetization is constitutively defined in the current configuration (Kankanala and Triantafyllidis, 2004), while it has no particular physical meaning in the undeformed configuration. Any attempt to use such a Lagrangian measure for the magnetization as an independent variable can lead to nonphysical measures of the latter in the current configuration. Such is the case for the **FM** model, originating by such a pull-back operation.

Finally, neglecting the background magnetic energy, an assumption typically made for simplicity of the analysis, may only be made in specific cases involving slender structures that are pre-magnetized uniformly and subjected to uniformly applied magnetic fields or with specific gradients. Even then, the reduced models may be able to predict accurately the mechanical response of the material or structure but, by construction, are incomplete as also recently discussed in Dorfmann and Ogden (2024) and thus incapable of describing the resulting magnetic response and its evolution during the loading process.

We further note that the observed stretch-independent magnetization response in *h*-MREs is also a feature of the most common incompressible, isotropic or chain-type particle-filled *s*-MREs; this was shown unambiguously in the earlier work of Danas et al. (2012) and a considerable effort to take it into account was made in their modeling approach, as well as in subsequent models (Lefèvre et al., 2017, 2019; Mukherjee et al., 2020). However, caution must be exercised, as anisotropic (Danas, 2017) or ferrofluid-filled (Lefèvre et al., 2017) *s*-MREs may exhibit different magnetization susceptibilities depending on the applied stretch, yet their saturation response was shown to be independent of the underlying microstructure but only a linear function of the magnetization saturation and volume fraction of the particles. This suggests that incompressible *h*-MREs created using such different inclusions may still exhibit a stretch-independent response near the fully pre-magnetized state. Yet, further studies are necessary to confirm or disprove this hypothesis and potential universal result especially for very soft matrices and isotropic or anisotropic microstructures.

In closing, it is important to acknowledge that the present study focused on the magneto-elastic description of *h*-MREs without considering viscoelastic effects. To obtain a comprehensive description of these materials, one has to incorporate mechanical dissipative effects. Although some efforts have been made in this direction (Garcia-Gonzalez, 2019; Garcia-Gonzalez and Landis, 2020; Rambausek et al., 2022; Lucarini et al., 2022; Gonzalez-Saiz and Garcia-Gonzalez, 2023; Stewart and Anand, 2023), it is evident that further experimental and theoretical investigations are necessary to fully characterize the viscoelastic response of *h*-MREs and develop more accurate models.

We hope that the present study will yield a better understanding and further the design of programmable materials and soft robots comprising components made of *h*-, *s*-, or hybrid MRE materials.

CRediT authorship contribution statement

Kostas Danas: Writing – review & editing, Writing – original draft, Methodology, Investigation, Funding acquisition, Formal analysis, Conceptualization. **Pedro M. Reis:** Writing – review & editing, Methodology, Investigation, Formal analysis, Conceptualization.

Declaration of competing interest

The authors declare that they have no known competing financial interests or personal relationships that could have appeared to influence the work reported in this paper.

Data availability

Data will be made available on request.

Acknowledgments

The authors would like to thank Prof. Dipayan Mukherjee for his careful reading of the manuscript and his valuable suggestions. K.D. would like to acknowledge support from the European Research Council (ERC) under the European Union's Horizon 2020 research and innovation program (grant agreements 636903 and 101081821).

References

Bassiouny, E., Ghaleb, A., Maugin, G., 1988. Thermodynamical formulation for coupled electromechanical hysteresis effects–I. Basic equations. Internat. J. Engrg. Sci. 26, 1279–1295. http://dx.doi.org/10.1016/0020-7225(88)90047-x.

Bednarek, S., 2006. The giant linear magnetostriction in elastic ferromagnetic composites within a porous matrix. J. Magn. Magn. Mater. 301, 200–207. http://dx.doi.org/10.1016/j.jmmm.2005.05.041, URL: https://www.sciencedirect.com/science/article/pii/S0304885305006633.

Brown, W.F., 1963. Micromagnetics. Vol. 18, Interscience Publishers.

Brown, W.F., 1966. Magnetoelastic Interactions. Vol. 9, Springer.

Bustamante, R., Dorfmann, A., Ogden, R., 2008. On variational formulations in nonlinear magnetoelastostatics. Math. Mech. Solids 13, 725–745. http://dx.doi.org/10.1177/1081286507079832.

Chang, X., Hallais, S., Danas, K., Roux, S., 2023. Peakforce afm analysis enhanced with model reduction techniques. Sensors 23, http://dx.doi.org/10.3390/s23104730, URL: https://www.mdpi.com/1424-8220/23/10/4730.

Cowley, M.D., Rosensweig, R.E., 1967. The interfacial stability of a ferromagnetic fluid. J. Fluid Mech. 30, 671–688. http://dx.doi.org/10.1017/S0022112067001697, URL: https://www.cambridge.org/core/journals/journal-of-fluid-mechanics/article/interfacial-stability-of-a-ferromagnetic-fluid/B40DFB1706780F071CDC7B0DFBFF7FCD#article.

Danas, K., 2017. Effective response of classical, auxetic and chiral magnetoelastic materials by use of a new variational principle. J. Mech. Phys. Solids 105, 25–53. http://dx.doi.org/10.1016/j.jmps.2017.04.016.

Danas, K., 2024. Electro- and Magneto-Mechanics of Soft Solids. Springer, Cham, pp. 65–157, chapter 3. CISM International Centre for Mechanical Sciences.

Danas, K., Kankanala, S., Triantafyllidis, N., 2012. Experiments and modeling of iron-particle-filled magnetorheological elastomers. J. Mech. Phys. Solids 60, 120–138. http://dx.doi.org/10.1016/j.jmps.2011.09.006, URL: http://www.sciencedirect.com/science/article/pii/S0022509611001736.

Danas, K., Triantafyllidis, N., 2014. Instability of a magnetoelastic layer resting on a non-magnetic substrate. J. Mech. Phys. Solids 69, 67–83. http://dx.doi.org/10.1016/j.jmps.2014.04.003.

Daniel, L., Rekik, M., Hubert, O., 2014. A multiscale model for magneto-elastic behaviour including hysteresis effects. Arch. Appl. Mech. 84, 1307–1323. http://dx.doi.org/10.1007/s00419-014-0863-9.

Dorfmann, A., Ogden, R., 2003. Magnetoelastic modelling of elastomers. Eur. J. Mech. A Solids 22, 497–507. http://dx.doi.org/10.1016/s0997-7538(03)00067-6.

Dorfmann, A., Ogden, R., 2004. Nonlinear magnetoelastic deformations of elastomers. Acta Mech. 167, 13–28. http://dx.doi.org/10.1007/s00707-003-0061-2.

Dorfmann, A., Ogden, R., 2005. Some problems in nonlinear magnetoelasticity. Z. Angew. Math. Phys. ZAMP 56, 718–745. http://dx.doi.org/10.1007/s00033-004-4066-z.

Dorfmann, L., Ogden, R.W., 2024. Hard-magnetic soft magnetoelastic materials: Energy considerations. Int. J. Solids Struct. 294, 112789. http://dx.doi.org/10.1016/j.ijsolstr.2024.112789, URL: https://www.sciencedirect.com/science/article/pii/S0020768324001483.

Dorn, C., Bodelot, L., Danas, K., 2021. Experiments and numerical implementation of a boundary value problem involving a magnetorheological elastomer layer subjected to a nonuniform magnetic field. J. Appl. Mech. 88, http://dx.doi.org/10.1115/1.4050534.

Einstein, A., 1906. A new determination of molecular dimensions. Ann. Phys. 19, 289–306.

Eringen, A.C., Maugin, G., 1990. Electrodynamics of Continua I: Foundations and Solid Media. Springer-Verlag, New York.

Garcia-Gonzalez, D., 2019. Magneto-visco-hyperelasticity for hard-magnetic soft materials: theory and numerical applications. Smart Mater. Struct. 28, 085020. http://dx.doi.org/10.1088/1361-665x/ab2b05.

Garcia-Gonzalez, D., Landis, C.M., 2020. Magneto-diffusion-viscohyperelasticity for magneto-active hydrogels: Rate dependences across time scales. J. Mech. Phys. Solids 139, 103934. http://dx.doi.org/10.1016/j.jmps.2020.103934, URL: http://www.sciencedirect.com/science/article/pii/S0022509620301708.

Gebhart, P., Wallmersperger, T., 2022a. A constitutive macroscale model for compressible magneto-active polymers based on computational homogenization data: Part I — magnetic linear regime. Int. J. Solids Struct. 236–237, 111294. http://dx.doi.org/10.1016/j.ijsolstr.2021.111294, URL: https://www.sciencedirect.com/science/article/pii/S0020768321003747.

Gebhart, P., Wallmersperger, T., 2022b. A constitutive macroscale model for compressible magneto-active polymers based on computational homogenization data: Part II — magnetic nonlinear regime. Int. J. Solids Struct. 258, 111984. http://dx.doi.org/10.1016/j.ijsolstr.2022.111984, URL: https://www.sciencedirect.com/science/article/pii/S0020768322004371.

Gong, Q., Wu, J., Gong, X., Fan, Y., Xia, H., 2013. Smart polyurethane foam with magnetic field controlled modulus and anisotropic compression property. RSC Adv. 3, 3241–3248. http://dx.doi.org/10.1039/C2RA22824F.

Gonzalez-Saiz, E., Garcia-Gonzalez, D., 2023. Model-driven identification framework for optimal constitutive modeling from kinematics and rheological arrangement. Comput. Methods Appl. Mech. Engrg. 415, 116211. http://dx.doi.org/10.1016/j.cma.2023.116211, URL: https://www.sciencedirect.com/science/article/pii/S0045782523003353.

Hashin, Z., Shtrikman, S., 1963. A variational approach to the theory of the elastic behaviour of multiphase materials. J. Mech. Phys. Solids 11, 127–140. http://dx.doi.org/10.1016/0022-5096(63)90060-7.

Hill, R., 1950. The Mathematical Theory of Plasticity. Oxford at the Clarendon Press, Oxford.

Idiart, M., Moulinec, H., Castañeda, P.P., Suquet, P., 2006. Macroscopic behavior and field fluctuations in viscoplastic composites: second-order estimates versus full-field simulations. J. Mech. Phys. Solids 54, 1029–1063. http://dx.doi.org/10.1016/j.jmps.2005.11.004, URL: http://www.sciencedirect.com/science/article/pii/S0022509605002188.

James, R., Kinderlehrer, D., 1993. Theory of magnetostriction with applications to tbxdy1-xfe2. Philos. Mag. B 68, 237–274.

Kalina, K.A., Brummund, J., Metsch, P., Kästner, M., Borin, D.Y., Linke, J.M., Odenbach, S., 2017. Modeling of magnetic hystereses in soft mres filled with ndfeb particles. Smart Mater. Struct. 26, 105019. http://dx.doi.org/10.1088/1361-665x/aa7f81.

Kankanala, S., Triantafyllidis, N., 2004. On finitely strained magnetorheological elastomers. J. Mech. Phys. Solids 52, 2869–2908. http://dx.doi.org/10.1016/j.jmps.2004.04.007.

Karush, W., 1939. Minima of functions of several variables with inequalities as side constraints. URL: http://pi.lib.uchicago.edu/1001/cat/bib/4111654.

Klinkel, S., 2006. A phenomenological constitutive model for ferroelastic and ferroelectric hysteresis effects in ferroelectric ceramics. Int. J. Solids Struct. 43, 7197–7222. http://dx.doi.org/10.1016/j.ijsolstr.2006.03.008.

Kuhn, H.W., Tucker, A.W., 1951. Nonlinear programming. In: Berkeley Symp. on Math. Statist. and Prob.. pp. 481–492, URL: https://projecteuclid.org/ebooks/berkeley-symposium-on-mathematical-statistics-and-probability/Proceedings-of-the-Second-Berkeley-Symposium-on-Mathematical-Statistics-and/chapter/Nonlinear-Programming/bsmsp/1200500249.

Kuruzar, M., Cullity, B., 1971. The magnetostriction of iron under tensile and compressive tests. Int. J. Magn. 1, 323–325. http://dx.doi.org/10.1007/s00419-014-0863-9.

Landis, C.M., 2002. Fully coupled, multi-axial, symmetric constitutive laws for polycrystalline ferroelectric ceramics. J. Mech. Phys. Solids 50, 127–152. http://dx.doi.org/10.1016/s0022-5096(01)00021-7.

Lee, E.H., 1969. Elastic-plastic deformation at finite strains. J. Appl. Mech. 36, 1–6. http://dx.doi.org/10.1115/1.3564580, arXiv:https://asmedigitalcollection.asme.org/appliedmechanics/article-pdf/36/1/1/5449476/1_1.pdf.

Lefèvre, V., Danas, K., Lopez-Pamies, O., 2017. A general result for the magnetoelastic response of isotropic suspensions of iron and ferrofluid particles in rubber, with applications to spherical and cylindrical specimens. J. Mech. Phys. Solids 107, 343–364. http://dx.doi.org/10.1016/j.jmps.2017.06.017.

Lefèvre, V., Danas, K., Lopez-Pamies, O., 2019. Two families of explicit models constructed from a homogenization solution for the magnetoelastic response of mres containing iron and ferrofluid particles. Int. J. Non-Linear Mech. http://dx.doi.org/10.1016/j.ijnonlinmec.2019.103362, URL: http://www.sciencedirect.com/science/article/pii/S0020746219306237.

Linnemann, K., Klinkel, S., Wagner, W., 2009. A constitutive model for magnetostrictive and piezoelectric materials. Int. J. Solids Struct. 46, 1149–1166. http://dx.doi.org/10.1016/j.ijsolstr.2008.10.014.

Lopez-Pamies, O., Goudarzi, T., Danas, K., 2013. The nonlinear elastic response of suspensions of rigid inclusions in rubber: II– simple explicit approximation for finite-concentration suspensions. J. Mech. Phys. Solids 61, 19–37. http://dx.doi.org/10.1016/j.jmps.2012.08.013.

Lucarini, S., Moreno-Mateos, M., Danas, K., Garcia-Gonzalez, D., 2022. Insights into the viscohyperelastic response of soft magnetorheological elastomers: Competition of macrostructural versus microstructural players. Int. J. Solids Struct. 256, 111981. http://dx.doi.org/10.1016/j.ijsolstr.2022.111981, URL: https://www.sciencedirect.com/science/article/pii/S0020768322004346.

Luo, H., Hooshmand-Ahoor, Z., Danas, K., Diani, J., 2023. Numerical estimation via remeshing and analytical modeling of nonlinear elastic composites comprising a large volume fraction of randomly distributed spherical particles or voids. Eur. J. Mech. A Solids 101, 105076. http://dx.doi.org/10.1016/j.euromechsol.2023.105076, URL: https://www.sciencedirect.com/science/article/pii/S0997753823001687.

Moreno, M., Gonzalez-Rico, J., Lopez-Donaire, M., Arias, A., Garcia-Gonzalez, D., 2021. New experimental insights into magneto-mechanical rate dependences of magnetorheological elastomers. Composites B 224, 109148. http://dx.doi.org/10.1016/j.compositesb.2021.109148, URL: https://www.sciencedirect.com/science/article/pii/S1359836821005291.

Moreno-Mateos, M.A., Danas, K., Garcia-Gonzalez, D., 2023. Influence of magnetic boundary conditions on the quantitative modelling of magnetorheological elastomers. Mech. Mater. 184, 104742. http://dx.doi.org/10.1016/j.mechmat.2023.104742, URL: https://www.sciencedirect.com/science/article/pii/S0167663623001886.

Moreno-Mateos, M.A., Gonzalez-Rico, J., Nunez-Sardinha, E., Gomez-Cruz, C., Lopez-Donaire, M.L., Lucarini, S., Arias, A., Muñoz-Barrutia, A., Velasco, D., Garcia-Gonzalez, D., 2022a. Magneto-mechanical system to reproduce and quantify complex strain patterns in biological materials. Appl. Mater. Today 27, 101437. http://dx.doi.org/10.1016/j.apmt.2022.101437, URL: https://www.sciencedirect.com/science/article/pii/S2352940722000762.

Moreno-Mateos, M.A., Hossain, M., Steinmann, P., Garcia-Gonzalez, D., 2022b. Hybrid magnetorheological elastomers enable versatile soft actuators. NPJ Comput. Mater. 8, http://dx.doi.org/10.1038/s41524-022-00844-1.

Mukherjee, D., Bodelot, L., Danas, K., 2020. Microstructurally-guided explicit continuum models for isotropic magnetorheological elastomers with iron particles. Int. J. Non-Linear Mech. 103380. http://dx.doi.org/10.1016/j.ijnonlinmec.2019.103380.

Mukherjee, D., Danas, K., 2019. An evolving switching surface model for ferromagnetic hysteresis. J. Appl. Phys. 125, 033902. http://dx.doi.org/10.1063/1.5051483.

Mukherjee, D., Danas, K., 2022. A unified dual modeling framework for soft and hard magnetorheological elastomers. Int. J. Solids Struct. 257, 111513. http://dx.doi.org/10.1016/j.ijsolstr.2022.111513, URL: https://www.sciencedirect.com/science/article/pii/S0020768322000725, special Issue in the honour Dr Stelios Kyriakides.

Mukherjee, D., Rambausek, M., Danas, K., 2021a. An explicit dissipative model for isotropic hard magnetorheological elastomers. J. Mech. Phys. Solids 151, 104361. http://dx.doi.org/10.1016/j.jmps.2021.104361.

Mukherjee, D., Rambausek, M., Danas, K., 2021b. Abaqus UEL subroutine for hard and soft magnetorheological elastomers. http://dx.doi.org/10.5281/zenodo.4588578.

Pelteret, J.P., Davydov, D., McBride, A., Vu, D.K., Steinmann, P., 2016. Computational electro-elasticity and magneto-elasticity for quasi-incompressible media immersed in free space. Internat. J. Numer. Methods Engrg. 108, 1307–1342. http://dx.doi.org/10.1002/nme.5254, URL: http://onlinelibrary.wiley.com/doi/10.1002/nme.5254/abstract.

Psarra, E., Bodelot, L., Danas, K., 2017. Two-field surface pattern control via marginally stable magnetorheological elastomers. Soft Matter 13, 6576–6584. http://dx.doi.org/10.1039/c7sm00996h.

Psarra, E., Bodelot, L., Danas, K., 2019. Wrinkling to crinkling transitions and curvature localization in a magnetoelastic film bonded to a non-magnetic substrate. J. Mech. Phys. Solids 133, 103734. http://dx.doi.org/10.1016/j.jmps.2019.103734.

Rambausek, M., Danas, K., 2021. Bifurcation of magnetorheological film–substrate elastomers subjected to biaxial pre-compression and transverse magnetic fields. Int. J. Non-Linear Mech. 128, 103608. http://dx.doi.org/10.1016/j.ijnonlinmec.2020.103608.

Rambausek, M., Mukherjee, D., Danas, K., 2021. Supplementary material to "A computational framework for magnetically hard and soft viscoelastic magnetorheological elastomers". http://dx.doi.org/10.5281/zenodo.5543516.

Rambausek, M., Mukherjee, D., Danas, K., 2022. A computational framework for magnetically hard and soft viscoelastic magnetorheological elastomers. Comput. Methods Appl. Mech. Engrg. 391, 114500. http://dx.doi.org/10.1016/j.cma.2021.114500, URL: https://www.sciencedirect.com/science/article/pii/S0045782521007064.

Rambausek, M., Schöberl, J., 2023. Curing spurious magneto-mechanical coupling in soft non-magnetic materials. Internat. J. Numer. Methods Engrg. 124, 2261–2291. http://dx.doi.org/10.1002/nme.7210, URL: https://onlinelibrary.wiley.com/doi/abs/10.1002/nme.7210. arXiv:https://onlinelibrary.wiley.com/doi/pdf/10.1002/nme.7210.

Ren, Z., Hu, W., Dong, X., Sitti, M., 2019. Multi-functional soft-bodied jellyfish-like swimming. Nature Commun. 10, http://dx.doi.org/10.1038/s41467-019-10549-7.

Sano, T.G., 2022b. Reduced theory for hard magnetic rods with dipole–dipole interactions. J. Phys. A 55, 104002. http://dx.doi.org/10.1088/1751-8121/ac4de2.

Sano, T.G., Pezzulla, M., Reis, P.M., 2022a. A kirchhoff-like theory for hard magnetic rods under geometrically nonlinear deformation in three dimensions. J. Mech. Phys. Solids 160, 104739. http://dx.doi.org/10.1016/j.jmps.2021.104739, URL: https://www.sciencedirect.com/science/article/pii/S0022509621003458.

Schümann, M., Borin, D., Huang, S., Auernhammer, G., Müller, R., Odenbach, S., 2017. A characterisation of the magnetically induced movement of ndfeb-particles in magnetorheological elastomers. Smart Mater. Struct. 26, 095018. http://dx.doi.org/10.1088/1361-665x/aa788a.

Sharma, B.L., Saxena, P., 2020. Variational principles of nonlinear magnetoelastostatics and their correspondences. Math. Mech. Solids 26, 1424–1454. http://dx.doi.org/10.1177/1081286520975808.

Stepanov, G.V., Borin, D.Y., Bakhtiiarov, A.V., Storozhenko, P.A., 2017. Magnetic properties of hybrid elastomers with magnetically hard fillers: rotation of particles. Smart Mater. Struct. 26, 035060. http://dx.doi.org/10.1088/1361-665X/aa5d3c.

Stewart, E.M., Anand, L., 2023. Magneto-viscoelasticity of hard-magnetic soft-elastomers: Application to modeling the dynamic snap-through behavior of a bistable arch. J. Mech. Phys. Solids 179, 105366. http://dx.doi.org/10.1016/j.jmps.2023.105366, URL: https://www.sciencedirect.com/science/article/pii/S0022509623001709.

Wang, X., Gordaninejad, F., 2009. A new magnetorheological fluid–elastomer mount: phenomenological modeling and experimental study. Smart Mater. Struct. 18, 095045. http://dx.doi.org/10.1088/0964-1726/18/9/095045.

Yan, D., Abbasi, A., Reis, P.M., 2021. A comprehensive framework for hard-magnetic beams: Reduced-order theory, 3d simulations, and experiments. Int. J. Solids Struct. 111319. http://dx.doi.org/10.1016/j.ijsolstr.2021.111319, URL: https://www.sciencedirect.com/science/article/pii/S0020768321003978.

Yan, D., Aymon, B.F., Reis, P.M., 2023. A reduced-order, rotation-based model for thin hard-magnetic plates. J. Mech. Phys. Solids 170, 105095. http://dx.doi.org/10.1016/j.jmps.2022.105095, URL: https://www.sciencedirect.com/science/article/pii/S0022509622002721.

Zhang, Y., Ma, Y., Yu, J., Gao, H., 2023. Non-contact actuated snap-through buckling of a pre-buckled bistable hard-magnetic elastica. Int. J. Solids Struct. 281, 112413. http://dx.doi.org/10.1016/j.ijsolstr.2023.112413, URL: https://www.sciencedirect.com/science/article/pii/S0020768323003104.

Zhao, R., Kim, Y., Chester, S.A., Sharma, P., Zhao, X., 2019. Mechanics of hard-magnetic soft materials. J. Mech. Phys. Solids 124, 244–263. http://dx.doi.org/10.1016/j.jmps.2018.10.008.